Dalton Transactions

PERSPECTIVE

View Article Online
View Journal | View Issue

Cyclic peptide marine metabolites and Cu^{II}

Cite this: *Dalton Trans.*, 2014, **43**, 1935

Peter Comba,*[a] Nina Dovalil,[a] Lawrence R. Gahan,[b] Graeme R. Hanson[c] and Michael Westphal[a]

Received 25th September 2013,
Accepted 30th October 2013

DOI: 10.1039/c3dt52664j

www.rsc.org/dalton

Cyclic pseudo-peptides derived from marine metabolites of the genus *Lissoclinum bistratum* and *Lissoclinum patella* have attracted scientific interest in the last two decades. Their structural properties and solution dynamics have been analyzed in detail, elaborate synthetic procedures for the natural products and synthetic derivatives developed, the biosynthetic pathways studied and it now is possible to produce them biosynthetically. Initially, these macrocyclic ligands were studied due to their medicinal and pharmaceutical potential – some of the isolated cyclic pseudo-peptides show high cytotoxic and antiviral activity. A major focus in the last decade has been on their Cu^{II} coordination chemistry, as a number of studies have indicated that dinuclear Cu^{II} complexes of cyclic peptides may be involved in the ascidians' metabolism, and this is the focus of the present review.

1. Introduction

Marine life is remarkably different from its terrestrial counterpart and it is no surprise that the molecules and metabolites isolated from marine organisms differ strikingly from those of terrestrial sources. The interest in molecules from marine organisms increased considerably in the 1960s, when numerous metabolites were found to have excellent antiviral and cytotoxic properties.[1–6] In just 10 years (between 1977 and

[a]*Universität Heidelberg, Anorganisch-Chemisches Institut, INF 270, D-69120 Heidelberg, Germany. E-mail: peter.comba@aci.uni-heidelberg.de; Fax: +49-6221-546617*
[b]*School of Chemistry and Molecular Biosciences, The University of Queensland, Brisbane, Queensland 4072, Australia*
[c]*Centre for Advanced Imaging, The University of Queensland, Brisbane, Queensland 4072, Australia*

Peter Comba

Peter Comba (born in 1953) obtained a diploma in chemistry and chemical education from ETH Zürich and a PhD with Professor Werner Marty from the Université de Neuchâtel. He then was a research fellow with Professor Alan Sargeson at the Australian National University, Canberra, before returning to Switzerland (Université de Lausanne, with Professor André Merbach, and Universität Basel), and taking up his present position as Professor of Chemistry at the Universität Heidelberg, Germany. He is interested in fundamental transition metal coordination chemistry, involving ligand design and synthesis, preparative coordination chemistry, spectroscopy as well as theoretical and computational inorganic chemistry, with projects in bioinorganic and medicinal inorganic chemistry, molecular magnetism and molecular catalysis.

Nina Dovalil

Nina Dovalil (born in 1982) obtained her diploma from the University of Heidelberg and a joint PhD from the University of Heidelberg and the University of Queensland. Her diploma thesis focused on the synthesis of functionalized patellamide derivatives as potential model systems for purple acid phosphatases. During her PhD she studied the influence of the stereochemistry and incorporated heterocycles on the Cu^{II} coordination chemistry of patellamide derivatives.

1987), approximately 2500 molecules were isolated from marine organisms.[7,8] To date the medicinal interest in invertebrates has led to the extraction of approximately 10 000 metabolites many of which show pharmaceutical potential.[9–18] Among the particularly well-studied organisms are sea squirts (*ascidians*), especially the genera *Lissoclinum patella* and *L. bistratum*, which are specifically highlighted in this perspective. *Ascidians* are sessile animals and remain firmly attached to substrates, such as rocks and shells. Their name is derived from the Greek word *askidion*, which means "leather bottle" and describes their physical appearance, a sac-like body structure with a tough outer "tunic" made of the polysaccharide tunicin which, compared to other tunicates, leads to a rather rigid "exoskeleton".[8] The alkaloids, especially cyclic peptides, extractable from *L. patella* and *L. bistratum* have attracted scientific interest for more than two decades, as they provide a wide range of cyclic peptides, based on unusual amino acids and with unusual structures and properties.[8–16,19]

Ascidians harbor an obligate symbiont, *Prochloron* sp., which, it is thought, might produce the cyclic peptides.[20,21] Through photosynthesis, *Prochloron* is an extremely important nutrient for their hosts.[22–24] Oxazoline-, thiazole-, and thiazoline-based cyclic pseudo-hepta- and pseudo-octapeptides, *e.g.* lissoclinamides,[25–29] patellamides,[30–32] and ascidiacyclamide[33,34] can be extracted from *L. patella*; *L. bistratum* on the other hand provides oxazoline-based cyclic pseudo-hexapeptides such as westiellamide[35,36] and bistratamide A–H (Scheme 1).[17,37–40] In the cyclic peptides, heterocyclic moieties alternate with D- and L-amino acid residues in the peptide sequence. The heterocycles are formally the condensation product of threonine or cysteine residues with the preceding amide functionality. The lack of imidazole heterocycles in the cyclic pseudo peptides is presumably due to the fact that diaminopropanoic acid, formally the amine analogue of serine, is not available in the ribosome.[41,42] Structurally, the peptides resemble 21-azacrown-7 and 24-azacrown-8 structures that are highly preorganized for the coordination of metal ions. The observation that, despite the biotoxicity of Cu^{II}, its concentration in the *ascidians* is roughly 10^4 times higher than in the surrounding sea water, has fostered the interest in the macromolecule's metal ion, and especially Cu^{II} coordination chemistry.[34,43–59]

The focus of this perspective is on the Cu^{II} coordination chemistry of the *L. patella* and *L. bistratum* cyclic peptides and a series of synthetic analogues. Structure and dynamics of the metal-free ligands and their applications are also reviewed. A summary of the biosynthesis and synthetic approaches towards cyclic peptide synthesis can be found elsewhere.[18,21,48,53,56,60–68] Specifically, we will discuss here structures, dynamics and reactivities of the Cu^{II} complexes and recent developments with respect to the question of what their biological function might be.

2. Cyclic pseudo-peptides

2.1. Structures and dynamics

Solid state and solution studies of the conformations of azole-based[69] marine cyclic peptides provide valuable insights into the factors which may affect the reactivities and the biological functions of these interesting molecules (see Fig. 1 and 2, see Schemes 1 and 2 for the structural formulae).[19,27,70–81] Usually, all protons of the peptide NH groups point towards the center of the macrocyclic ring and the peptide carbonyl functions

Lawrence R. Gahan

Lawrence Gahan (born in 1949) obtained a degree in chemistry and a PhD from La Trobe University, Melbourne, Australia. After postdoctoral positions in the United States and England he was a research fellow in the Research School of Chemistry at the Australian National University, Canberra, Australia, with Professor Alan Sargeson. Following a position at Monash University, Melbourne, he moved to the University of Queensland in Brisbane, Australia, in 1984, where he is currently a Professor of Chemistry. He is interested in transition metal coordination chemistry and bioinorganic chemistry.

Graeme R. Hanson

Graeme Hanson (born in 1955) obtained a BSc (Hons) degree in chemistry and a PhD from La Trobe University, Melbourne, Australia. Subsequently, he was a research fellow with Prof. Bert Vallee at the Center for Biophysical and Biochemical Sciences and Medicine, Harvard University and with Professor John Pilbrow in the Department of Physics at Monash University. He moved to The University of Queensland as a lecturer in Chemistry and then joined the Centre for Magnetic Resonance, which has evolved into the Centre for Advanced Imaging. He was promoted to full Professor in 2003 and is a fellow of the Royal Australian Chemical Institute. His interests lie in the experimental and theoretical aspects of EPR spectroscopy and their application in biological inorganic chemistry.

towards the outside, such that the amino acid side chains adopt pseudo-axial positions. Residues with identical stereochemistry face to the same side of the macrocycle reference plane, *e.g.*, all valine residues of the C_3-symmetrical westiellamide *H₃wa* are in *S** configuration and therefore face to one side (see Fig. 1d).

The heterocyclic moieties of cyclic pseudo-hexapeptides are almost coplanar in the case of incorporation of azoline rings (partially reduced azole, one instead of two double bonds in the heterocycle), *e.g.* oxazoline or thiazoline, whereas in the case of azole-containing peptides, the heterocyclic moieties of the macrocycle are arranged in a cone-like structure (see Fig. 1 and 2).[82] The dihedral angle χ[N_{amide}–C_α–C_{azole}–X] (see Fig. 3 for abbreviations) can be used to express the extent of deviation from planarity (χ = 180° in case of planarity). It has been shown that χ depends on the azole system and the size of the amino acid side chains:[81] the relative energy as a function of χ was calculated by approximate density functional theory (DFT) for the reference system with a chiral amino acid coupled to an azole moiety. A plot of the calculated energies is given in Fig. 3. The energy profile reflects the flexibility of the specific reference systems and reveals possible reasons for different conformations obtained for the various metal-free macrocycles. The energy profiles of the imidazole and oxazole reference systems with a small side chain (Fig. 3, left) exhibit two minima between 0° and 200°, *i.e.* 90° and 150° for imidazole, and 60° and 170° for oxazole, respectively. The small thiazole reference system, on the other hand, has three energetically similar minima at 30°, 80° and 160°, respectively, suggesting that thiazole-containing macrocycles are more flexible.

The energy profiles change significantly when a sterically demanding side chain is introduced (Fig. 3, right): the larger *tert*-butyl groups increase the activation barrier for the rotation along the dihedral angle χ, leading to a shift of the minima in the profile – especially dihedral angles between 120° and 200° are affected. Each energy profile only has one minimum in the range of 100° to 150°: 149° for the oxazole-, 129° for the thiazole-, and 104° for the imidazole *tert*-butyl reference systems, respectively.

Michael Westphal

Michael Westphal (born in 1984) obtained his diploma in chemistry from the University of Heidelberg. The focus of his diploma thesis was gold-catalyzed [3.3]-sigmatropic rearrangements. His PhD thesis, which he has just finished, concentrates on dicopper(II) complexes of patellamide analogues and their possible biological functions.

The computed preference of the azole systems for different dihedral angles corresponds to that found in the X-ray structures of the corresponding cyclic pseudo-hexapeptides (Fig. 1).[35,81] The reason for this difference was shown to be mainly of electronic origin: the $\pi(C_{azole}–N_{het})$ orbital of an imidazole ring is high in energy and, accordingly, preferably interacts with the $\sigma^*(C_\alpha–N_{amide})$ orbital. The optimum interaction between these two orbitals is at an angle of 90°, where the $\sigma^*(C_\alpha–N_{amide})$ orbital is oriented parallel to the $\pi(C_{azole}–N_{het})$ orbital. In contrast, the $\sigma^*(C_{azole}–N_{het})$ orbital of an oxazole ring is of low energy and therefore preferably interacts with the energetically high $\sigma(C_\alpha–C_\beta)$ and $\sigma(X_\alpha–H_\alpha)$ orbitals. This interaction has its optimum at an angle χ of 180°.[81]

The arrangement of heterocycles, linked by amides, enables an intramolecular network of bifurcated H-bonds, reflected in the average N_{amide}–H···N_{het} distances of 2.24 Å in the center of the molecule.[83] The planar conformation of the macrocycle is neither affected by the sign of chirality nor by substituents at C_α. *S**- and *R**-amino acid side chains are both directed pseudo-axially in opposite directions from the reference plane of the macrocycle.

The 18-membered cyclohexapeptides isolated from *L. bistratum* have a strong preference for a planar secondary structure, referred to as triangle conformation, that is adopted independently of the degree of saturation of the oxazole or thiazole rings (azole *vs*. azoline).[83] Intramolecular H-bond networks are also present in the 21-membered *Lissoclinum* pseudo-cycloheptapeptides, *e.g.*, the lissoclinamides and *cis*,*cis*-ceratospongamide, and the 24-membered *Lissoclinum* pseudo-cyclooctapeptides, *e.g.* the patellamides and ascidiacyclamide (Scheme 1). The cyclic pseudo-octapeptides are built up from an alternating sequence of Ser-, Thr- or Cys-derived azole rings, linked by hydrophobic amino acids. All *Lissoclinum* pseudo-octapeptides isolated so far have C_2- or C_1-symmetry. A substantial increase in flexibility compared to the cyclic pseudo-hexa- and pseudo-heptapeptides might be expected. However, analysis of the solid state and solution structures by X-ray crystallography,[27,73,74,84,85] ^{1}H-NMR spectroscopy,[19,33,72,85] DFT calculations[74] and molecular mechanics/Monte Carlo/molecular dynamics-based conformational analyses[27,72] indicated that there are four conformers which we summarize here in two types of conformations: the "saddle-shaped", sometimes also referred to as square, and the twisted "figure-of-eight" conformation (Fig. 4). NMR studies have shown that the pseudo-octapeptides adopt identical conformations in solution and the solid state.[26,33,36,66,72,86] In the "saddle-shaped" conformation all nitrogen atoms point towards the inside of the macrocycle, while the "figure-of-eight" conformation is characterized by intramolecular H-bonds, N–H···O=C and N–H···O_{oxa} (oxazoline ring), that lead to a rotation of the oxazoline rings such that the N_{oxa} atoms face the outside of the macrocycle.[27] Several reasons for the different preferences are discussed in the literature. One explanation is that a C_2-symmetric substitution results in a "saddle-shaped" conformation and, with decreasing symmetry, the twisted "figure-of-eight" form is preferred.[87] Another

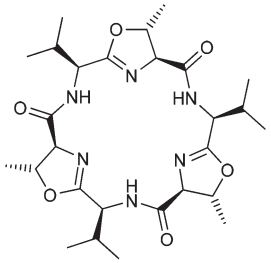

Westiellamide [a)]

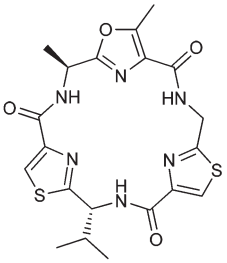

Nostocyclamide

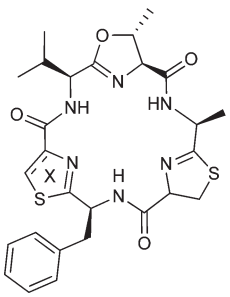

Bistratamide A, X = thiazoline
Bistratamide B, X = thiazole

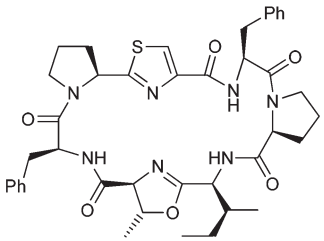

cis,cis-Ceratospongamide

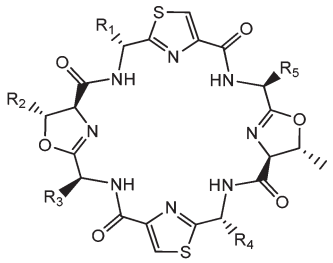

Patellamide A-G
Ascidiacyclamide

	R_1	R_2	R_3	R_4	R_5
Patellamide A	*D*-val	H	*L*-ile	*D*-val	*L*-ile
B	*D*-ala	Me	*L*-leu	*D*-phe	*L*-ile
C	*D*-ala	Me	*L*-val	*D*-phe	*L*-ile
D [a)]	*D*-phe	Me	*L*-ile	*D*-ala	*L*-ile
E	*D*-val	Me	*L*-val	*D*-phe	*L*-ile
F	*D*-phe	H	*L*-val	*D*-val	*L*-val
G	*D*-phe	Me	*L*-ile	*D*-ala	*L*-leu
Ascidiacyclamide [a)]	*D*-val	Me	*L*-ile	*D*-val	*L*-ile

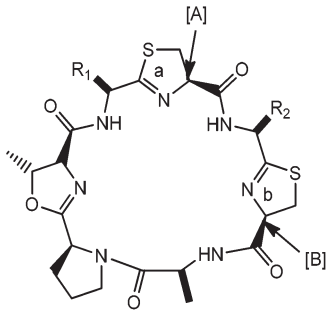

Lissoclinamide 1-10
Ulicyclamide

	R_1	R_2	*a*	*b*	*A/B*
Lissoclinamide 1	*L*-val	D-ile	thiazole	thiazole	-
2	*D*-ile	D-ala	thiazoline	thiazole	-
3	*D*-ile	L-ala	thiazolines	thiazolines	*R*
4	*L*-val	D-phe	thiazolines	thiazole	*R*
5	*L*-val	D-phe	thiazole	thiazole	-
6	*D*-val	D-phe	thiazolines	thiazole	*R*
7	val	phe	thiazoline	thiazolines	
8	val	phe	thiazoline	thiazole	
9	*L*-ile	D-val	thiazolines	thiazole	*R*
10	*L*-ile	L-ile	thiazolines	thiazoline	*R/R*
Ulicyclamide	*L*-ile	D-ala	thiazole	thiazole	

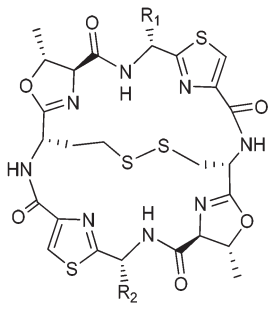

Ulithiacyclamide A-B

Ulithiacyclamide A	val	val
Ulithiacyclamide B	phe	val

Scheme 1 Structures of selected *L. patella* and *L. bistratum* cyclic peptides. [a] Abbreviations used in the text: patellamide D: H_4patD; ascidiacyclamide: H_4asc; westiellamide: H_3wa

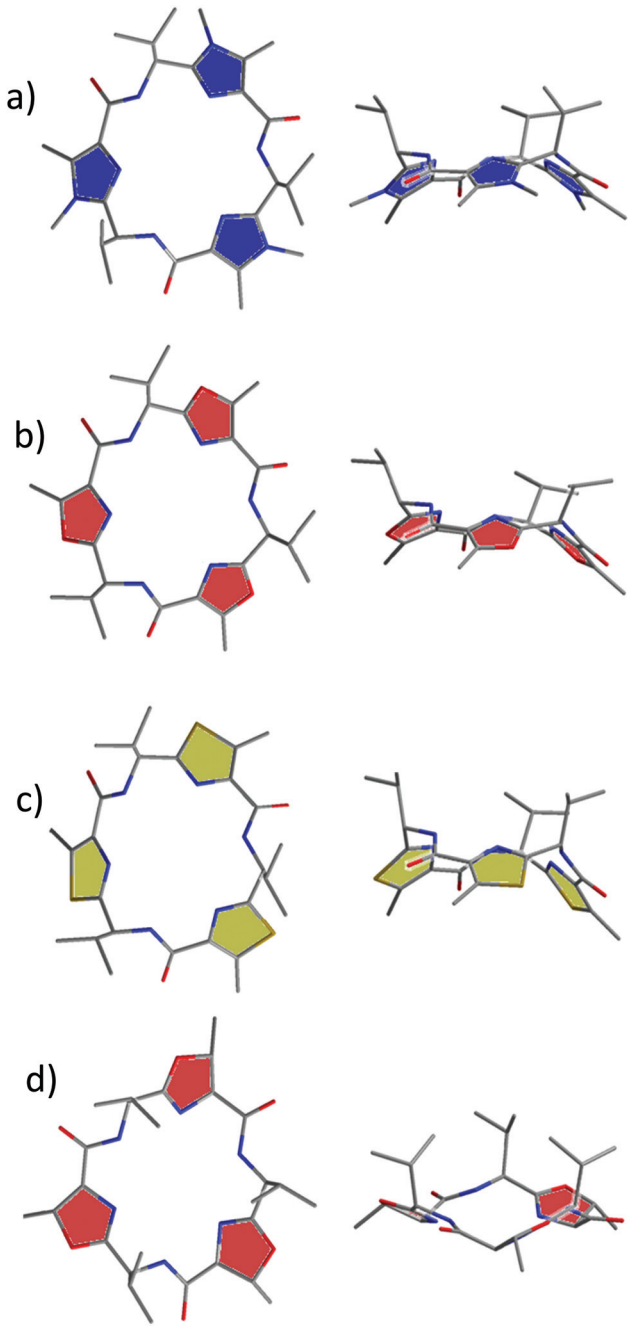

Fig. 1 Top (left) and side (right) views of the X-ray structures of the synthetic cyclic pseudo-hexapeptides H_3wa^{im} (a), H_3wa^{ox} (b), H_3wa^{thi} (c), and the natural system westiellamide H_3wa (d).[36,81] Color code: N = blue, O = red, C = grey, oxazole/oxazoline ring = red, thiazole ring = ochre, dimethylimidazole ring = blue.

possible explanation is based on the steric hindrance induced by the β-branched side chains (exclusively Val and Ile in H_4asc and H_4patA), and this potentially prevents the hydrophobic collapse of the system to the more compact "figure-of-eight" structure. More recent investigations have shown that a third factor, namely the incorporated heterocycles and the stereochemistry at C_α, also have substantial influence on the adopted conformation.[56,66]

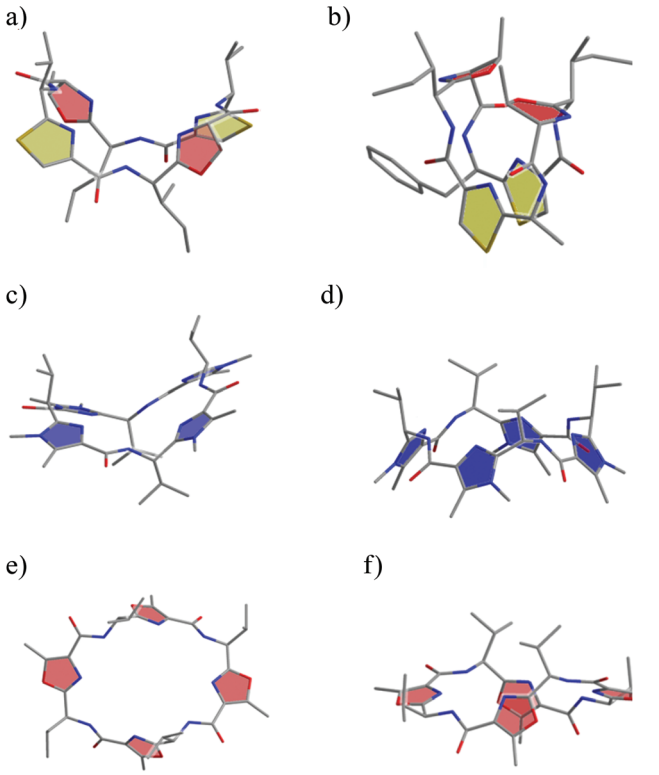

Fig. 2 Sideviews of the X-ray structures of (a) H_4asc;[84] (b) H_4patD;[27] (c) H_4pat^1;[56] (d) H_4pat^2;[56] and (e) top and (f) side view of the X-ray structure of H_4pat^3.[66] Color code: N = blue, O = red, C = grey, oxazole/-ine ring = red, thiazole ring = ochre, dimethylimidazole ring = blue. Reproduced by permission of Wiley-VCH from ref. 57.

We have studied the influence of the incorporated heterocycles and the stereochemistry at C_α on the adopted conformation of cyclic pseudo-octapeptides with a series of model systems and found that the adopted conformation not only depends on the symmetry but also on the configuration of the connecting amino acids and the incorporated heterocycles.[56,57] The comparison of the macrocycles H_4pat^{1-3} (Scheme 2) allows conclusions to be drawn about the correlation of the preferred solution structure of the metal-free macrocycles, structure and stability of the Cu^{II} complexes and reactivities related to carbonic anhydrase and phosphatase activities (see below).[56,57,88–90]

Symmetric cyclic pseudo-octapeptides adopt the square conformation and amino acid residues with identical C_α configuration face the same side of a macrocycle. The influence of C_α on the shape of the macrocycle is clearly visible upon examination of the X-ray structures of H_4pat^1 and H_4pat^2 (Fig. 2e and f). The dimethylimidazole rings of H_4pat^1 are oriented in a zig-zag fashion while the heterocycles of H_4pat^2 adopt a conical shape. H_4pat^3 can adopt two conformations in the solid state: one is identical to that of H_4pat^2, in the other two *trans*-disposed oxazole rings are rotated such that their ring systems are coplanar yet, in contrast to H_4patD, all nitrogen atoms are still oriented towards the center of the macrocycle. The heterocycles of the natural C_2-symmetric peptide H_4asc (Fig. 2a) are folded in zig-zag fashion, comparable to H_4pat^1.

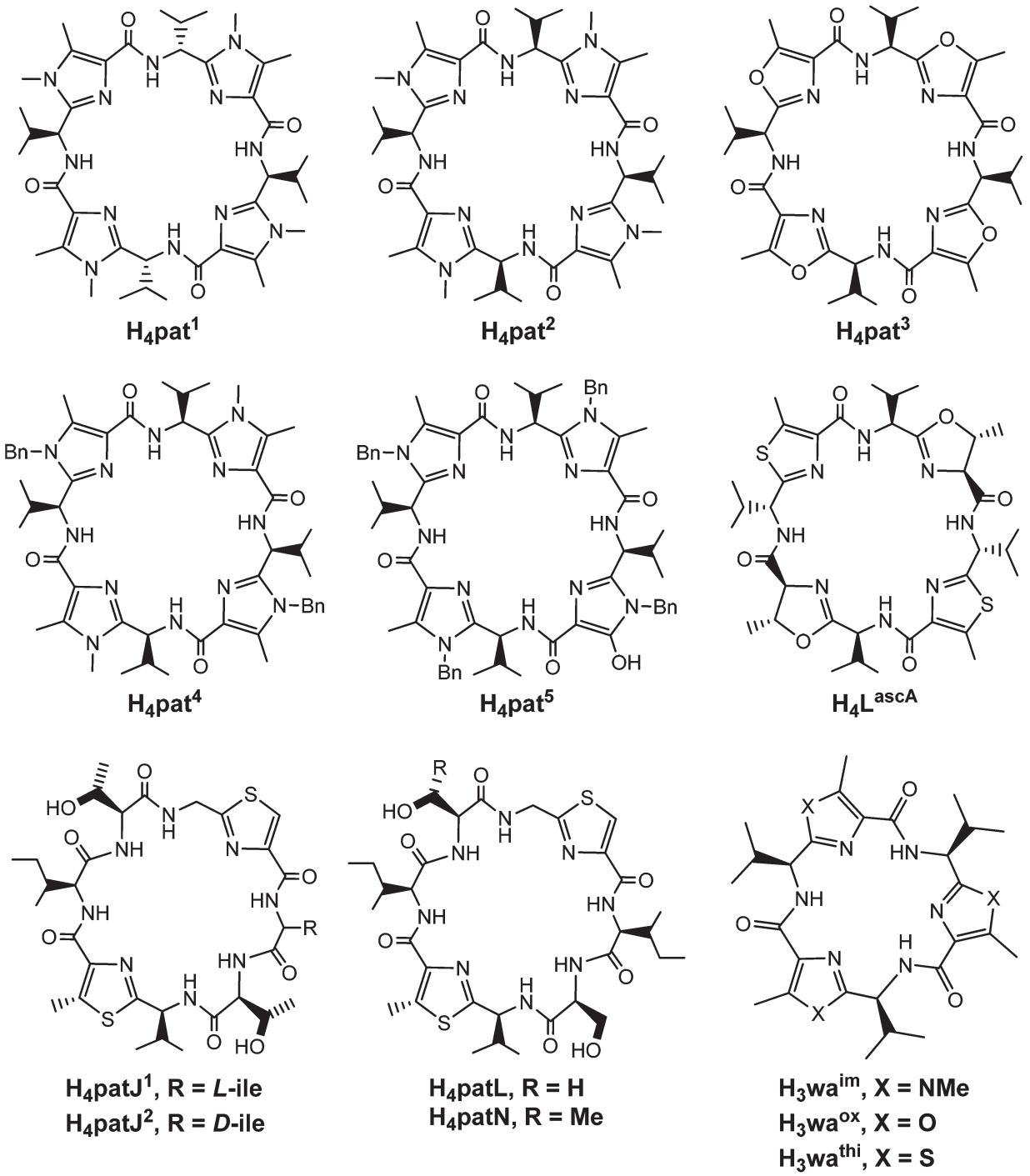

Scheme 2 Structures of the patellamide model systems H_4pat^{1-5}, the ascidiacyclamide analogue H_4L^{ascA}, the partly hydrolyzed model systems H_4patJ^1, H_4patJ^2, H_4patL, H_4patN, and the westiellamide analogues H_3wa^{het}.

The higher flexibility of the oxazoline rings in comparison to imidazole ($H_4pat^{1,2}$) and oxazole (H_4pat^3) results in a stronger twist of the heterocycles in H_4asc, compared to H_4pat^1 (Fig. 2). The figure-of-eight conformation adopted by asymmetric macrocycles (H_4patD, Fig. 2b) demands a higher flexibility of the macrocyclic backbone, as the N_{oxa} nitrogen atoms face towards the outside of the macrocycle and the thiazole rings are parallel. The synthetic symmetric macrocycles H_4pat^{1-3} and the natural peptide ascidiacyclamide have comparable distances of their N_{het} atoms but a strikingly different orientation of the heterocycles. The higher rigidity of the imidazoles of H_4pat^1 in combination with an alternating configuration at C_α leads to a somewhat more shielded cavity of H_4pat^1, compared to those of H_4asc, H_4patD, and $H_4pat^{2,3}$. H_4asc and H_4patD have a stronger twist of the heterocycles which enlarges the accessibility of the cavity, while the identical configuration

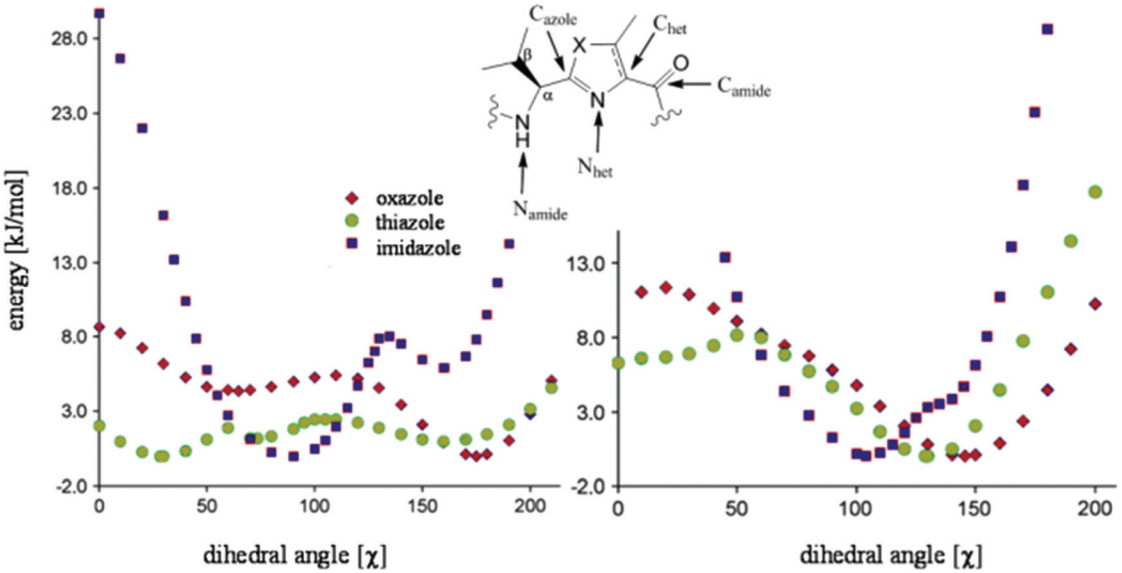

Fig. 3 Abbreviations and building blocks of natural and synthetic cyclic peptides used for DFT-based (G03, B3LYP/6-31g**) energy profiles (adopted from ref. 81) of oxazole, thiazole and imidazole reference systems for cyclic pseudo-peptides in relation to the dihedral angle χ;[81,82] left: small side-chain (iso-propyl); right: bulky side-chain (*tert*-butyl).

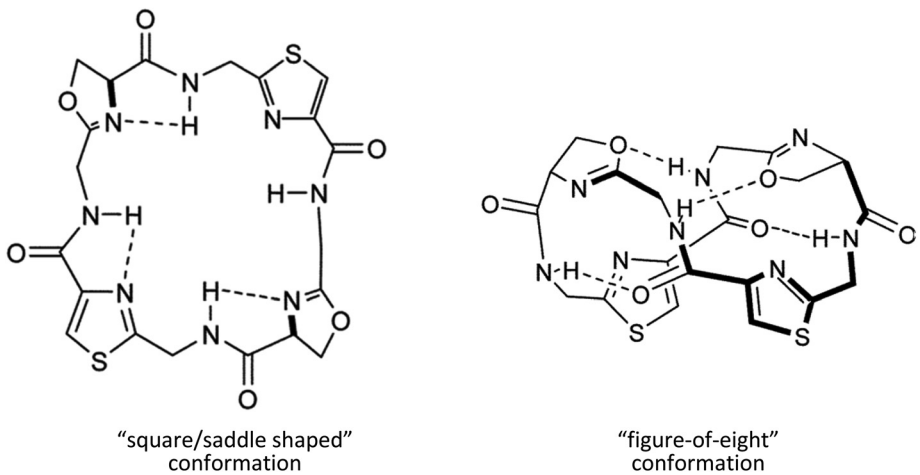

Fig. 4 Conformations of cyclic octapeptides: square/saddle shaped (left) and figure-of-eight (right). Reproduced by permission of Wiley-VCH from ref. 57.

at all C_α sites in H_4pat^2 and H_4pat^3 leads to a shielded and an unshielded side of the macrocycle.

2.2. Function and applications

The biological function of the cyclic pseudo-octapeptides is unknown. Due to the significant amount of metal ion accumulation in invertebrates[91] – specifically copper in *L. patella* – and due to the suitability of the cyclic peptide ligands for Cu^{II} (see below), it might be assumed that the natural function of the patellamide macrocycles involves Cu^{II} coordination, but not even this is a fact. The cyclic peptides and their Cu^{II} complexes might be cofactors in enzymes[43] and assume the typical functions of copper enzymes, *i.e.* electron transfer and oxygen activation. Another possible function of the macrocycles is their involvement in Cu^{II} transport, storage or detoxification.[43,92] Oxygen activation has been suggested as a possible biological role,[43,91,92] but due to the open coordination sites and rather low reduction potentials,[89] this does not seem to be a probable role except if the pseudo-peptides are prosthetic groups in proteins. CO_2 hydration (carbonic anhydrase activity),[23,34,43,56,57,90,93,94] and phosphoester hydrolysis (phosphatase activity)[88] have recently been proposed as possible biological functions, and this will be discussed in detail below.

Due to the known cytotoxic, antibacterial, antineoplastic and antiviral activities of the metal-free cyclic pseudo-peptides, medicinal and pharmaceutical applications have been studied extensively[13,17,18,44,95,96] and still are a driving force for cyclic peptide chemistry. The cyclic pseudo-peptides' use as macrocyclic ligands in transition metal coordination chemistry has been another focus of *Lissoclinum*-derived cyclic peptides, and

this will be reviewed in detail in the next section. The hydrogen bond donating and accepting properties of the alternating amide and azole groups makes the macrocycles also suitable receptors for anions, and this has been studied in some detail.[66,97,98]

Lissoclinum-derived and other synthetic cyclic peptides have been used as platforms for applications in molecular recognition.[97,99] Synthetic C_2 and C_3 symmetric macrocycles (see Scheme 3) were prepared for the selective coordination of anions – where significant stabilities and selectivities were achieved and interpreted on the basis of DFT calculations,[83,98,100] the enantioselective coordination of chiral organo-ammonium ions with selectivities of up to 87 : 13,[101] and as a novel class of C_3-symmetric cylindrical and conical container molecules, based on chiral glutamic acid and lysine-derived thiazole amino acids (also given in Scheme 3).[102]

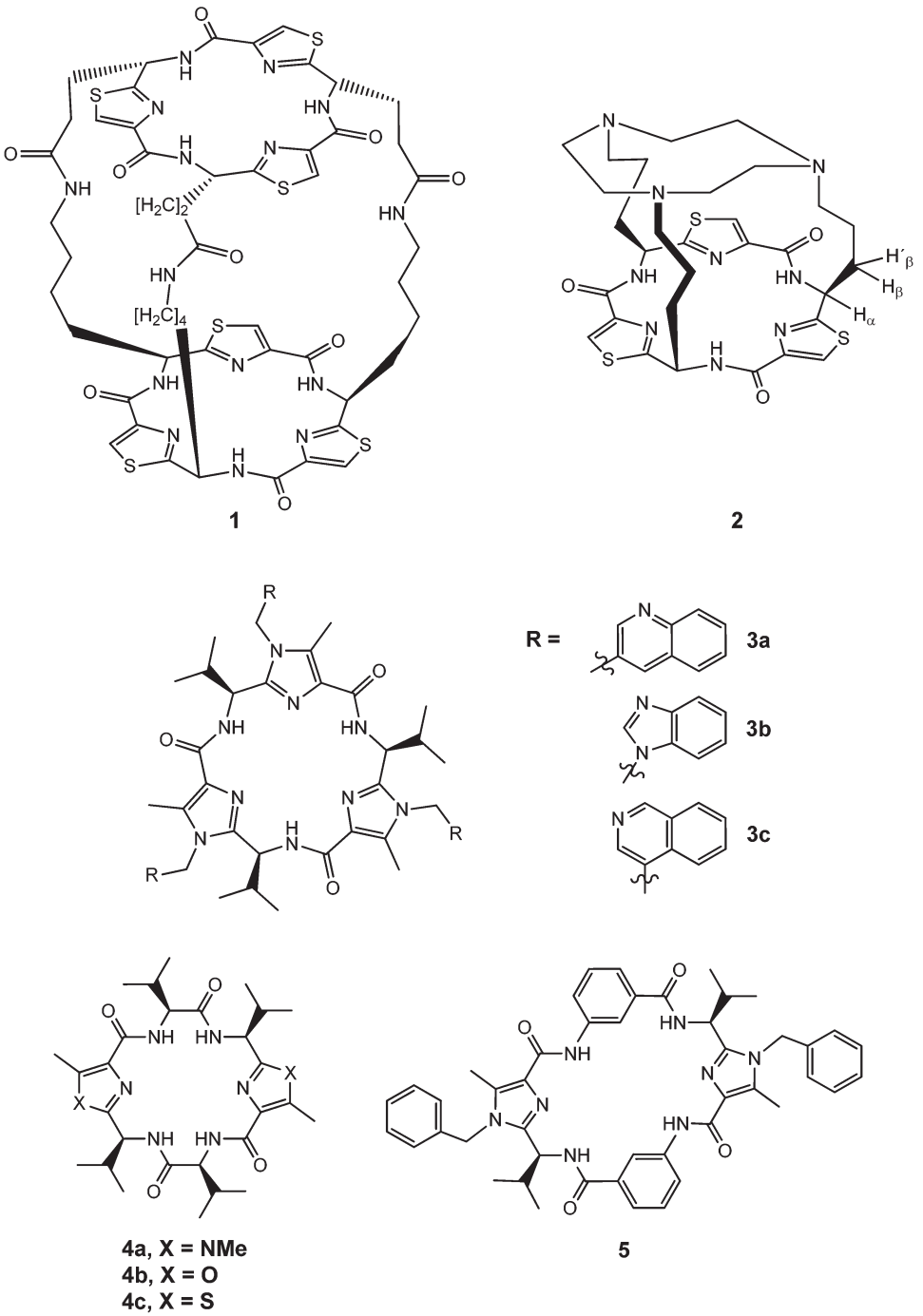

Scheme 3 C_3-symmetric container molecules **1**, **2**;[102] C_3-symmetric (**3**) and C_2-symmetric imidazole-based receptors (**4**, **5**) for enantiomeric recognition of primary ammonium salts.[98,101]

Cyclic pseudo-peptides, in particular the pseudo-hexapeptides derived from westiellamide and the C_2-symmetrical derivatives depicted in Scheme 3, have been shown to provide valuable scaffolds for supramolecular chemistry,[99,103] where exciting developments with novel molecular switches, motors and devices have emerged.[104] Particularly interesting recent examples based on cyclic peptide scaffolds are those of unidirectional switches,[105] a unidirectional motor,[106] a 4-stroke motor,[107] and a light-induced chirality switch.[108]

3. Metal binding to *Lissoclinum* peptides and synthetic models

The strong preference for a planar secondary structure of the patellamide-type pseudo-cyclopeptides and the presence of a cavity with appropriately placed nitrogen and oxygen donors in these macrocyclic structures has been noted as an optimal arrangement for chelation.[43,56,57,84,89,92,109] Coupled with this, the observation of the capacity of *L. patella* to concentrate a range of metal ions, including but not limited to Cu^{II}, led to extensive efforts over a considerable period to understand the role of the cyclic peptides in metal ion complexation and accumulation. Initial reasons for investigation included the coordination chemistry of the individual metal ions, understanding the electronic structures, stabilities and selectivity with particular metal ions, and recent efforts have been directed increasingly towards reactivities to elucidate the possible biological functions of these peptides and complexes.[34,43–47,49,61,67,94,110–113] There is a distinct difference between various species with respect to the heterocycles involved in the cyclic peptides, and this must lead to differences in the corresponding transition metal coordination chemistry, specifically also in terms of electronic structures, stabilities and reactivities and therefore might have some influence in the biological activity. The *L. bistratum* derived macrocycles include oxazoline-based cyclic pseudo-hexapeptides (*e.g.* westiellamide, bistratamide A–H) while those from *L. patella* include oxazoline-, thiazole- and thiazoline-based cyclic pseudo-hepta- and pseudo-octapeptides, (*e.g.* lissoclinamides, patellamides and ascidiacyclamide), see Scheme 1.

3.1. *Lissoclinum bistratum* derived peptides

Initial studies on the metal ion complexation of westiellamide reported the formation of an unusual Ag_4 cluster complex (see Fig. 5):[47] three of the silver(I) ions are disposed in a *pseudo*-trigonal arrangement about Ag1 and are sandwiched between two H_3wa macrocycles (westiellamide). The central silver ion Ag1 is coordinated in a distorted octahedral arrangement by the carbonyl oxygen atoms of the two H_3wa ligands. The usual conformation of the cyclic pseudo-hexapeptide is strongly twisted in this silver cluster: in order to coordinate to the central silver(I) ion Ag1, the carbonyl groups of westiellamide are rotated towards the inside of the ring, thus flipping the macrocycle and rotating the amide nitrogens such that they face the outside of the macrocycle (see above for the relative

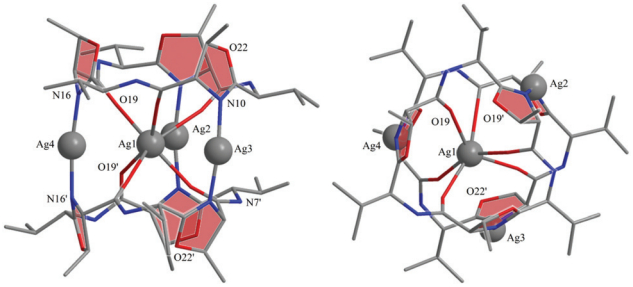

Fig. 5 X-ray structure of the Ag_4 cluster of westiellamide.[47]

stability of the various conformers of the metal-free peptide ligands).

NMR titrations in [D_4]methanol indicated that H_3wa is selective for Ag^I, *i.e.* only "weak interactions" were observed with Li^I, Na^I, K^I, Cu^I, Mg^{II}, Cd^{II}, Hg^{II}, Ni^{II}, Cu^{II}, Fe^{II}, Fe^{III}, Au^{III} and Ce^{III}, while the association constant in the Ag^I 2 : 1 complex was reported to be $>10^5$. Extensive work on the H_3wa^n/Cu^{II} system in methanol, also including the synthetic analogues H_3wa^{im}, H_3wa^{thi} and H_3wa^{ox} (see Schemes 1 and 2), using titrations of ligand solutions with Cu^{II} and/or base (OMe^-), vis-NIR, CD, ESI-MS and EPR spectroscopy, spectra simulations, combined with DFT-based molecular modeling, and microcalorimetry (ITC), indicated that mono- as well as dinuclear Cu^{II} complexes are formed with stability constants of approx. 10^5, *i.e.* similar to those of the patellamide-type cyclic pseudo-octapeptides (see Table 1).[54,55] The structures of these complexes depend on the electronic properties and, specifically also on the flexibilities of the heterocycles, and yield two structural types each for the mono- and dinuclear Cu^{II} complexes, respectively (see Fig. 6).

The synthetic macrocycles H_3wa^{im}, H_3wa^{thi} and H_3wa^{ox} have the westiellamide (H_3wa) backbone, derived from L-valine amino acid residues, and differ only in their heterocyclic donor group, *i.e.* oxazoline, oxazole, imidazole and thiazole (see Schemes 1 and 2). Importantly, this leads to differences in shape and flexibility of the macrocycles (see section on structures and dynamics of the metal-free cyclic pseudo-peptides), with the oxazoline-based natural macrocycle westiellamide H_3wa being the most flexible, and this is the reason for the subtle structural differences of the Cu^{II} complexes (see Fig. 6) and thermodynamic properties (see Table 1).

In the mononuclear complexes of the synthetic ligands, each Cu^{II} is coordinated by three nitrogen atoms of the macrocycle and the coordination sphere is completed by solvent molecules (see Fig. 6).[54] Two of the nitrogen donors originate from azole rings and one from the connecting amide group, forming the usual N_{het}–N_{amide}–N_{het} bonding motif. The deprotonation is metal ion assisted and takes place at relatively low pH values – Cu^{II} is known to be able to deprotonate amide nitrogen atoms in oligopeptides at pH ≈ 4–5).[114–116] The protons that are released upon coordination of Cu^{II} acidify the solution, and make the addition of base mandatory in order to achieve complete complexation. In the natural environment,

Table 1 Complex stabilities of cyclic peptide ligands with various metal ions

Metal ion	Cyclic peptide	Method	K_1	K_2	Reference
Cu^{II}	Patellamide A	CD	2.00×10^4	7.76×10^2	44, 113
		MS	3.31×10^4	1.00×10^4	44
Cu^{II}	Patellamide B	CD	3.02×10^5	2.29×10^2	113
Cu^{II}	Patellamide C	CD	6.70×10^4		44
		MS	6.31×10^4	6.03×10^3	44
Cu^{II}	Patellamide E	CD	1.51×10^4		113
Zn^{II}	Ascidiacyclamide	NMR, CD	1.00×10^3		113
Zn^{II}	Patellamide A	CD	3.02×10^4	1.00×10^3	44
		MS	2.82×10^3	3.89×10^3	44
Zn^{II}	Patellamide B	CD	3.02×10^4	1.91×10^1	113
Zn^{II}	Patellamide C	CD	1.78×10^4	8.13×10^2	44
		MS	2.40×10^3	2.57×10^3	44
Zn^{II}	Patellamide E	CD	7.94×10^4	2.00×10^1	113
Cu^{II}	Lissoclinamide 9	CD	1.41×10^4	1.26×10^2	45
Cu^{II}	H_4pat^1	ITC	1.71×10^6 [a]		89
Cu^{II}	H_4pat^2	ITC	4.03×10^4 [a]		89
Cu^{II}	H_4pat^3	ITC	2.27×10^5 [a]		89
Cu^{II}	H_4pat^4	ITC	1.43×10^5 [a]		89
Cu^{II}	H_4pat^5	ITC	1.50×10^5 [a]		89
Cu^{II}	H_3wa^{im}	ITC	2.03×10^5	0.67×10^5	56
Cu^{II}	H_3wa^{ox}	ITC	3.31×10^5	4.14×10^5	56
Cu^{II}	H_3wa^{thi}	ITC	1.97×10^5	0.50×10^5	56
Ca^{II}	Ascidiacyclamide	NMR	7.94×10^2		76
Ca^{II}	Patellamide D	NMR, CD	7.94×10^2		76

[a] ITC data indicate cooperative binding of two metal ions,[48,53,56,56,57,89,133] and structural studies indicate that this is due to preorganization of the second coordination site by binding of the first Cu^{II} ion to the ligand,[56] resulting in one K value for both binding sites.

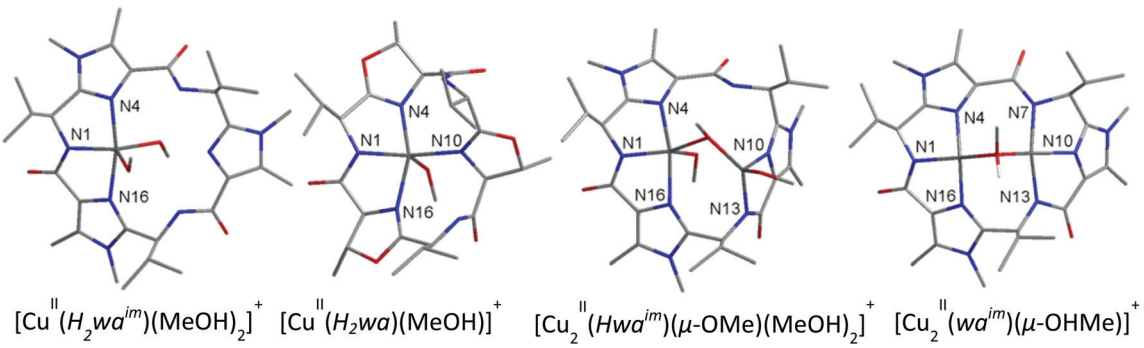

Fig. 6 Solution structures (DFT combined with EPR spectroscopy) of the Cu^{II} complexes of westiellamide-type cyclic pseudo-hexapeptides.[54] Reproduced by permission of Wiley-VCH from ref. 54.

the slight basicity and constant pH of ~8 of seawater provides the conditions for coordination of Cu^{II} to the N_{het}–N_{amide}–N_{het} pocket and supports the assumption that the metabolic role of the cyclic peptides is related to metal ion coordination, specifically with Cu^{II}. Interestingly, the structure of the mononuclear H_3wa complex is strikingly different. The increased flexibility of the oxazoline heterocycles allows the third heterocycle also to be coordinated, leading to a distorted square pyramidal coordination geometry with a N_{het}–N_{amide}–N_{het}–N_{het} donor set and an axial MeOH completing the coordination sphere (note that this follows from a thorough analysis of the EPR spectra supported by DFT calculations).[54] This leads to an increased stability of the mononuclear structure and largely prevents formation of dinuclear complexes. Two isomers are observed for these dinuclear compounds (see Fig. 6), and these differ by the donor set provided for the second Cu^{II} center: N_{het}–N_{amide}–OMe^- *vs.* N_{amide}–N_{het}–N_{amide}.

For the methylimidazole-based macrocycle H_3wa^{im} the detailed analysis of the solution structure and electronic properties of the mono- and dicopper(II) complex was extended with pulsed electron nuclear double resonance (ENDOR), hyperfine sublevel correlation resonance (HYSCORE) and magnetic circular dichroism spectroscopy (MCD), combined with a detailed DFT study, involving the careful validation of the theoretical setup (functional and basis set)[59] – the computation of spin Hamiltonian parameters is notoriously difficult.[117] While the analysis of the ENDOR spectra of $[Cu^{II}(H_2wa^{im})]^+$ confirmed the bonding motif (N_{het}–N_{amide}–N_{het}), the three nitrogen nuclei are magnetically inequivalent. HYSCORE spectra revealed delocalization of the unpaired

electron onto the remote nitrogen of the imidazole ring. A DFT comparison of the singly occupied orbital for the Cu^{II} complexes of all pseudo-hexapeptide ligands, $[Cu^{II}(H_2wa^{im})]^+$, $[Cu^{II}(H_2wa^{thi})]^+$, $[Cu^{II}(H_2wa^{ox})]^+$ and $[Cu^{II}(H_2wa)]^+$ showed significant delocalization of the unpaired electron onto the heterocyclic ring in all cases.

The stability constants of the mono- and dinuclear Cu^{II} complexes of the westiellamide analogues were determined using isothermal titration calorimetry (ITC) and computed by standard fitting procedures.[55] It was found that the complexation behavior of the three synthetic analogues H_3wa^{im}, H_3wa^{thi} and H_3wa^{ox} was strikingly different from one another (see Table 1). In contrast to H_3wa^{im} and H_3wa^{thi}, H_3wa^{ox} does not only form mono- and dinuclear Cu^{II} complexes but also a macrocycle : Cu^{II} = 2 : 1 species in a preequilibrium, which leads to significant differences in the solution chemistry. This unusual coordination mode was confirmed by NMR, EPR and ESI-MS experiments (note that similar observations emerge for the pseudo-octapeptide Cu^{II} complexes discussed below; see Scheme 4 for the corresponding structural model). In this coordination mode, Cu^{II} is not coordinated to the usual N_{het}–N_{amide}–N_{het} binding site (see above) but interacts with the "outside" of the macrocycle *via* carbonyl oxygen atoms from the amide groups, with MeOH completing the coordination sphere. DFT calculations confirm this spectroscopically determined structure. Computational models also confirm the ITC-based thermodynamic observation that, for H_3wa^{ox}, the strain induced to the macrocyclic ligand backbone is larger for the coordination of the first Cu^{II} ion than for the second. The small conformational change needed for the coordination to the second Cu^{II} ion in H_3wa^{ox} facilitates the formation of dinuclear complexes. The cooperativity of H_3wa^{im} and H_3wa^{thi} was also observed in ITC experiments.[55]

3.2. *Lissoclinum Patella* derived peptides

3.2.1. Solution equilibria. Families of cyclic peptides were first isolated from *L. patella* in the 1980s with a range of compounds being identified and characterized.[84,118,119] Apart from the interesting medicinal properties of the metal-free ligands, the high concentration of Cu^{II} and a range of other metal ions in *ascidians*,[91] together with the structural similarity of the cyclic pseudo-peptides to aza-crown ethers, suggested that the peptides are tailor-made for binding to metal ions,[43] although direct evidence for complex formation was originally not available.[109] The potential for metal ion complexation by a range of marine metabolites, including those from *L. patella* was discussed in a 1993 review.[112] However, the limiting factor in metal ion complexation studies was (and partially still is) the availability of large enough amounts of the metabolites (ligands). In addition, an often not unambiguously solved question is,[47,112] whether the biological activity involves metal ion chelation – what exactly the biological activity is has not yet been studied in detail.

Initial quantitative investigations of the interactions of metal ions with a range of patellamides were undertaken using NMR, EPR, UV-vis-NIR and circular dichroism (CD) spectroscopy. For many reasons Cu^{II} usually was the metal ion of choice, driven to some extent by the spectroscopic advantages of the d^9 electronic configuration but also by the biological relevance of the metal ion. In some cases the complexation behavior with Zn^{II} and other metal ions was also investigated,[49,120,121] and the solution coordination chemistry of patellamides A, B, D and E, ascidiacyclamide and a number of cyclo-octapeptide analogues with Cu^{II} and Zn^{II} was investigated in some detail;[45,113,120,122,123] in addition, the interaction of Ca^{II} with ascidiacyclamide and patellamide D was also reported.[76] The potassium complex of a partially hydrolyzed ascidiacyclamide was structurally characterized (Fig. 7).[124] The binding constants for a series of cyclic peptides from *L. patella* and *L. bistratum* together with synthetic analogues are assembled in Table 1. The log $K_{1:1}$ binding constants generally lie in the range 3.5–5.5 for Cu^{II} and Zn^{II}; in some cases two binding events were observed, the second often at least one order of magnitude smaller than the first (except in cases where cooperativity is observed, *vide infra*). The observed complex stabilities were taken as support for the suggestion that the Cu^{II} complexes are biologically relevant.[120] For reactions with Zn^{II} the anion used and the pH were shown to have a significant influence on the complexation processes[122] – for Cu^{II} this obviously is also the case, see below.

Our main focus in the last decade has been on the Cu^{II} chemistry of synthetic analogues of the naturally occurring cyclic pseudo-octapeptides patellamide D and ascidiacyclamide.[125] Our original synthetic strategy involved the cyclization of the octapeptides with open ("hydrolyzed") oxazoline heterocycles (ligands *patN*, *patL*, *patJ*[1] and *patJ*[2], Scheme 2; the heterocycles of these ligands were not closed so far although this should be feasible).[48,53] These syntheses were quite tedious and did not yield sufficient quantities of the ligands for comprehensive studies of the solution coordination chemistry. However, based on ESI-MS, electronic (UV-vis-NIR and CD) and EPR spectroscopy, we have been able to fully characterize the main mono- and dinuclear species in solution. The stoichiometry generally is well defined by ESI-MS experiments and supported by CD and/or UV-vis-NIR titrations. The electronic transition energies have so far mainly been used in conjunction with qualitative ligand field arguments to support the structural assignments based on EPR spectroscopy. The experimental spectra, in combination with spectra simulations and molecular modeling to solve the solution structures of the weakly dipole–dipole coupled dicopper(II) systems have been extremely useful for the unambiguous structural characterizations. This approach uses the simulation of the EPR spectra with structural parameters (Cu···Cu distance and relative orientation of the two chromophores with respect to each other) in addition to the spin Hamiltonian parameters of the two Cu^{II} centers.[126,127] The structural parameters are also refined with molecular mechanics based molecular modeling, and this combination (MM-EPR) permits the unambiguous determination of the solution structures.[128] This method has been further developed to also include the DFT-based computation of the spin Hamiltonian parameters (MM-DFT-EPR),[129]

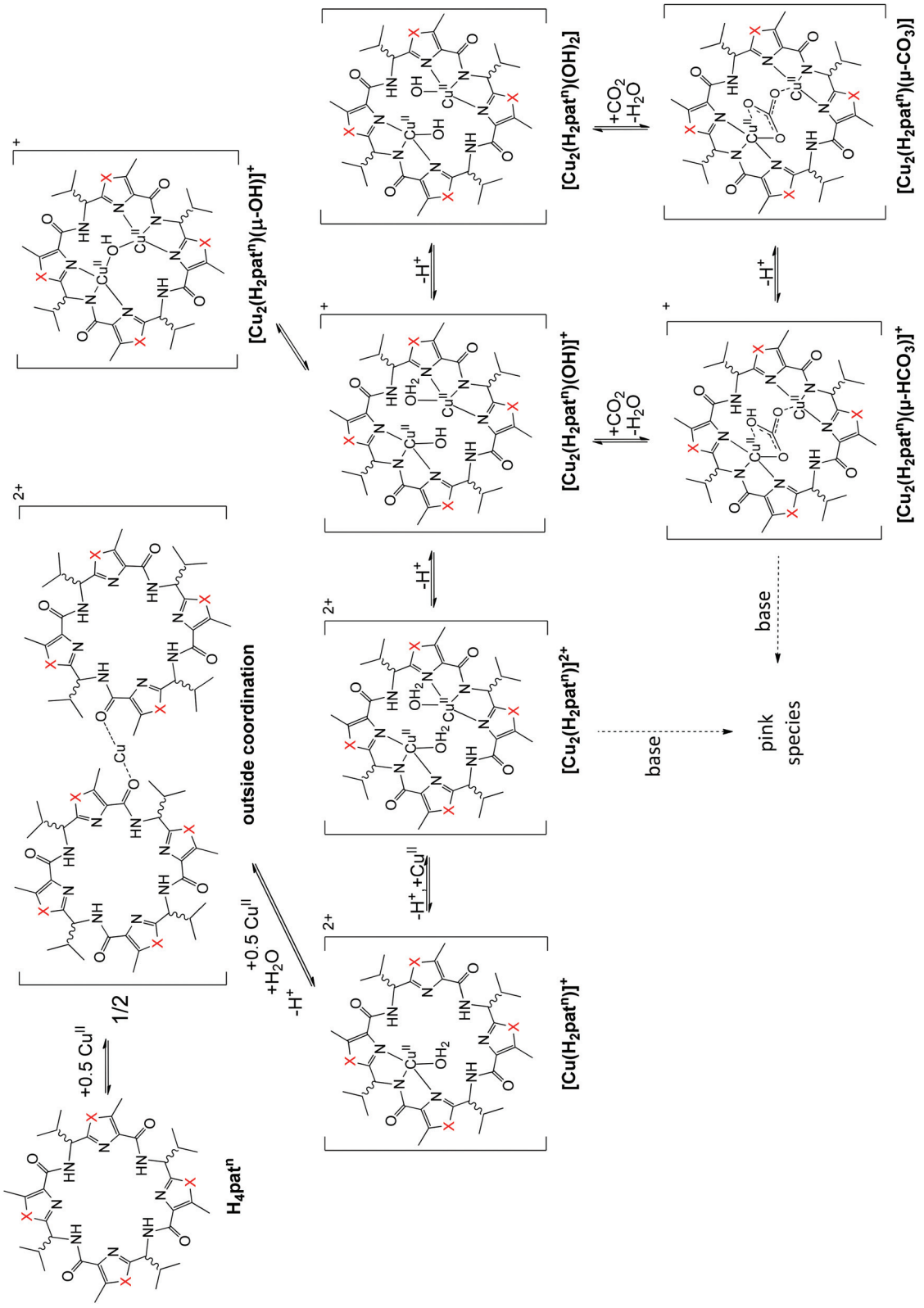

Scheme 4 Cu^{II} complexation equilibria of H_4pat^n.[57]

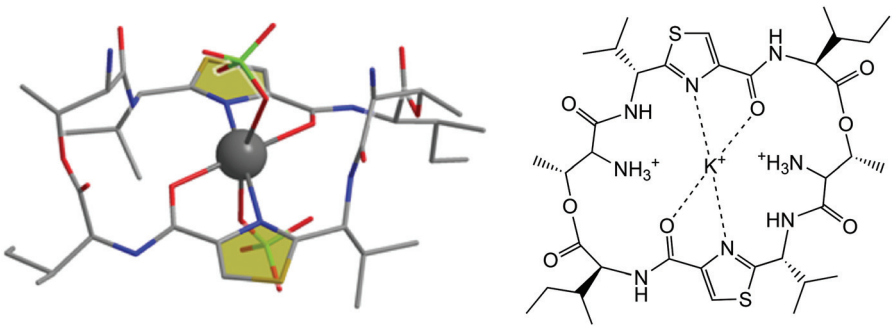

Fig. 7 X-ray (left) and chemical structure (right) of the potassium(I) complex of hydrolyzed ascidiacyclamide.[124]

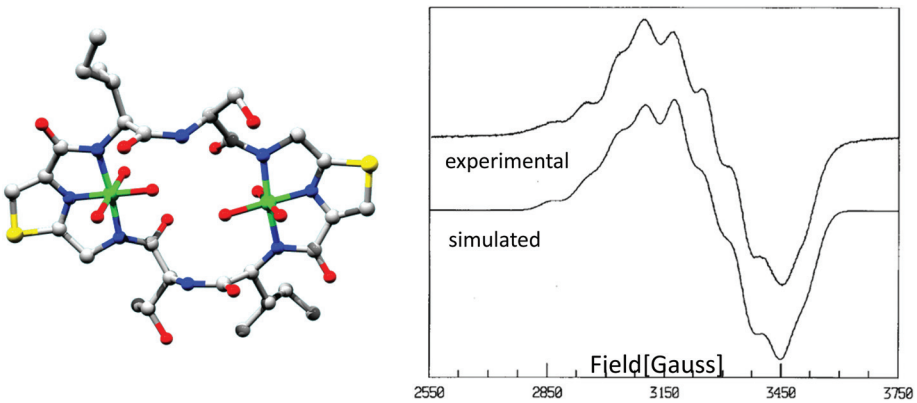

Fig. 8 Solution structure of the dicopper(II) complex of *H₄patN* (MM-EPR; green: Cu, blue: N, red: O, yellow: S, cyan: C).[48] Reprinted with permission from Inorganic Chemistry from ref. 48. Copyright 1998 by American Chemical Society.

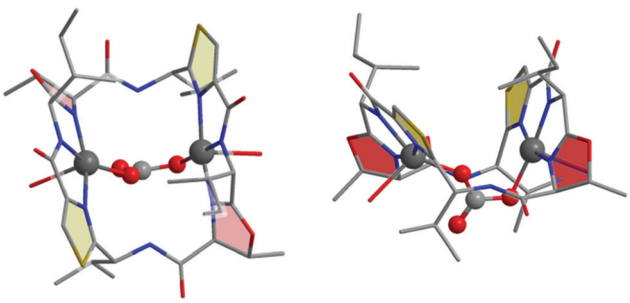

Fig. 9 Top and side view of $[Cu_2^{II}(H_2asc)(\mu\text{-}CO_3)]$ (X-ray structure).[34] Reproduced by permission of Wiley-VCH from ref. 57.

and more recently, additional parameters (exchange coupling *J* and zero-field splitting *D*) have also been considered in the spectral simulations, and their prediction is based on a range of quantum-chemical methods (see also section on the westiellamide-based macrocycles above).[54,130–132] The solution structures of the dicopper(II) complexes of *patN*, *patL*, *patJ*[1] and *patJ*[2] were solved by MM-EPR,[48,53] that of *patN* together with the experimental and simulated EPR spectrum are shown in Fig. 8. At the time this was the second structure of a Cu^{II} complex of an *L. patella* derived cyclic peptide (the other is that of $[Cu_2(H_2asc)(1,2\text{-}\mu\text{-}CO_3)(H_2O)_2]\cdot 2H_2O$, determined by single crystal X-ray crystallography,[34] shown in Fig. 9; see also Fig. 7 for the only other structure of a metal complex of this type of ligand available a decade ago.[124]

A new modular synthesis, with improved efficiency and variability[65,68,78] has helped to prepare a range of *L. patella* type cyclic pseudo-octapeptides with varying heterocyclic donor sets and configurations of the macrocycle side chains (*H₄pat*[1]–*H₄pat*[5], see Scheme 2), including ligands with an identical donor set and/or side-chain configurations as observed in the natural products.[56,57,89]

In all complexes of these cyclic pseudo-octapeptides, Cu^{II} is generally coordinated to two heterocyclic nitrogen atoms and a nitrogen of a deprotonated amide group, forming the usual N_{het}–N_{amide}–N_{het} bonding motif. The formation of the mono- and dinuclear Cu^{II} complexes involves a metal-ion assisted deprotonation (*vide supra*). Based on electronic absorption, CD and EPR spectral titrations, the following sequence of complexation reactions with Cu^{II} was proposed for patellamide D, with formation of a carbonato complex, similar to that observed with the dicopper(II) complex with ascidiacyclamide.[34,94]

$$[Cu(MeOH)]^{2+} + H_4patD + NEt_3 \rightarrow [Cu(H_3patD)]^{+} + NEt_3H^{+}$$

$$[Cu(H_3patD)]^{+} + [Cu(MeOH)]^{2+} + NEt_3 \rightarrow [Cu_2(H_2patD)]^{2+} + NEt_3H^{+}$$

$$[Cu_2(H_2patD)]^{2+} + NEt_3 \rightarrow [Cu_2(H_2patD)(OH)]^{+} + NEt_3H^{+}$$

$$[Cu_2(H_2patD)(OH)]^{+} + CO_2 \rightarrow [Cu_2(H_2patD)(CO_3)] + H_2O$$

Extensive studies with the series of the synthetic analogues H_4pat^1–H_4pat^5 as well as with *patN*, *patL*, *patJ*^{1} and *patJ*^{2} (see Scheme 2)[48,53,56,57,89] led to the general scheme of solution equilibria shown in Scheme 4. Note that (i) the preequilibrium with "outside coordination" of two macrocycles to one Cu^{II} center (see also section on the Cu^{II} chemistry of the pseudo-hexapeptides above) has so far only been observed with oxazole-based ligands. (ii) There are two isomers of the mono-hydroxo-dicopper(II) complexes, one with a terminal and one with a bridging hydroxide. Both have distinct structural properties (determined in solution by MM-EPR;[57] with H_4pat^1 we have been able to trap the hydroxo-bridged complex and solve the structure by X-ray crystallography.[56] (iii) There is one more species in equilibrium, a "pink species" which never has been fully characterized – it forms slowly from both the carbonato and the diaqua complexes upon addition of excess base;[53,56,57] for the reactivities discussed below it does however not seem to be of importance.

3.2.2. Structural properties. Cooperative binding of two Cu^{II} ions to the patellamide-type cyclic pseudo-octapeptides (see above, see Table 1)[48,53,56,57,89,133] was confirmed by computational and experimental structural work to be the result of a preorganization of the second binding site of the macrocycle by coordination to the first Cu^{II} ion.[56,57] For H_4pat^2 this is visualized in Fig. 10: the overlay of the computed and experimental structures of the metal-free ligand shows that the computational model used is appropriate (this is also confirmed by a comparison of the experimental and computed structures of $[(H_2pat^1)(\mu\text{-}OH)]^+$, see below); the overlay of the computed structures of the metal-free ligand and the mono-copper(II) complex indicates that significant structural rearrangement is required while the overlay of the mono- and dinuclear complexes shows that their structures are close to identical.[58]

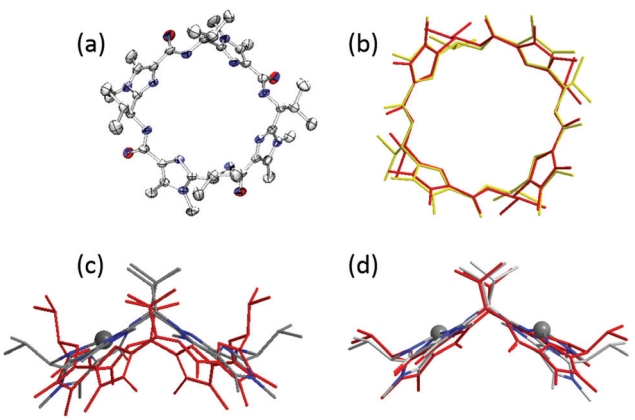

Fig. 10 (a) X-ray structure of H_4pat^2; (b) overlay of the X-ray structure of H_4pat^2 (red) with its DFT-optimized structure; (c) overlay of the DFT-optimized structures of H_4pat^2 (red) with its mononuclear Cu^{II} complex (color-coded); (d) overlay of the DFT-optimized structures of the mononuclear Cu^{II} complex of H_4pat^2 (red) with its dinuclear Cu^{II} complex (color-coded). Reprinted with permission from Inorganic Chemistry from ref. 56. Copyright 2011 by American Chemical Society.

The conformational analysis of the metal-free macrocycles revealed that it is not possible for H_4pat^1 to adopt a similar structure to those of H_4asc or H_4patD, as the incorporated dimethyl-imidazole rings introduce severe steric constraints (see also section on the ligand structures).[59] With H_4pat^1 and two equivalents of Cu^{II} at low base concentrations a dinuclear Cu^{II} aqua complex is formed $[Cu_2^{II}(H_2pat^1)(H_2O)]^{2+}$.[58] Alignment of the two Cu^{II} centers along the *magic angles* (θ = 54.7°, ϕ = 45.0°) eliminates the dipole–dipole contribution to the anisotropic exchange interaction, producing an "apparent mononuclear EPR spectrum". Addition of more than three equivalents of base leads to the formation of two structurally different hydroxo complexes, one with a terminal hydroxide, $[Cu_2^{II}(H_2pat^1)(OH)]^+$, the other with a hydroxo bridge, $[Cu_2^{II}(H_2pat^1)(\mu\text{-}OH)]^+$ (see Scheme 4). In the former complex the two Cu^{II} centers are in a similar orientation to that in the aqua complex, *i.e.* along the magic angles, while the formation of a hydroxo bridge leads to a reorientation of the Cu^{II} centers and the macrocyclic backbone, such that a typical dipole–dipole coupled EPR spectrum emerges.

As predicted by the simulated EPR spectra, the mono- and dinuclear Cu^{II} complexes of H_4pat^1 are found to have a distorted square pyramidal coordination geometry, where the equatorial donor atoms involve two imidazole nitrogens N_{het}, one amide nitrogen N_{amide}, and one oxygen of a coordinated water molecule. The apical Cu1–O2 distance is with 2.29 Å as expected (pseudo-Jahn–Teller distortion) significantly longer than that in the equatorial plane (Cu1–O1 = 2.04 Å). DFT analyses of the corresponding ligand conformations suggest that the ligand in the hydroxo-bridged complex is 25 kJ mol^{-1} more stable than the conformation in the mononuclear complex, and this again explains the preferred formation of dinuclear complexes (cooperativity, see above).

Comparison of the X-ray structures of H_4asc and its dinuclear carbonato-bridged complex with the DFT optimized and X-ray structures of H_4pat^1 and its hydroxo-bridged complex reveals structural similarities between the two systems but also important differences (see Fig. 11). Overlay of the structures of the metal-free macrocycles with those of their dinuclear Cu^{II} complexes illustrates the high degree of preorganization for the formation of the dinuclear complexes. The significant differences between the H_4asc and H_4pat^1 systems are primarily related to the tighter folding of the natural metal-free macrocycle compared to the imidazole-derived synthetic ligand, and the resulting differences in the relative orientation of the two Cu^{II} sites (distance and twist of the planes, see also Fig. 12 and 13 for a comparison of the structures of various dicopper(II) complexes). From the experimental and computed structures it emerges that the resulting structure of the ligand backbone and the two Cu^{II} sites in the case of H_4asc is well suited for a bridging carbonate (3-atom bridge, Cu···Cu = 4.3 Å), while with H_4pat^1 the dinuclear complex is preorganized for the much smaller hydroxo bridge (1-atom bridge, Cu···Cu =

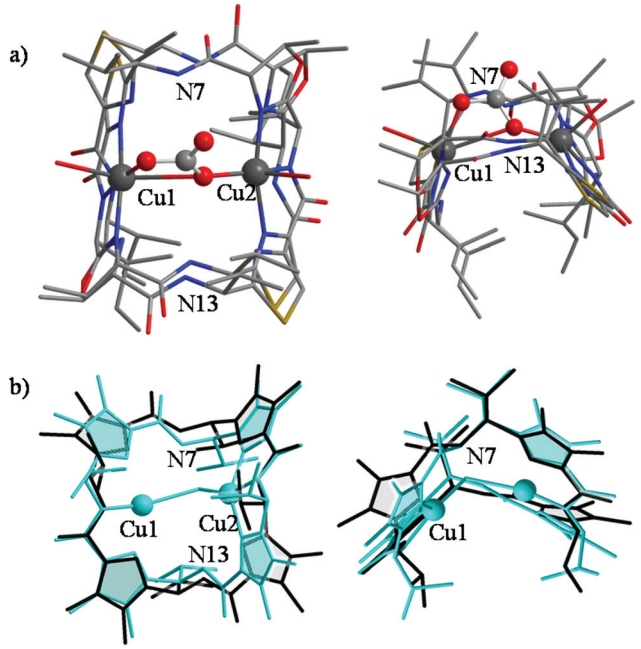

Fig. 11 Top (left) and side views (right) of the following overlay plots: (a) H_4asc and $[Cu_2^{II}(H_2asc)(\mu\text{-}CO_3)]$ (X-ray structures); (b) X-ray structure of H_4pat^1 (black) with its computed (G09, B3LYP/6-31g*/TZVP, turquoise) dinuclear Cu^{II} complex $[Cu_2^{II}(H_2pat^1)(\mu\text{-}OH)]^+$ (note that this structure is very similar to the corresponding X-ray structure, see Fig. 13; it has been optimized to obtain the relative strain induced to the ligand at the minimum of the potential energy surface). Reprinted with permission from Inorganic Chemistry from ref. 56. Copyright 2011 by American Chemical Society.

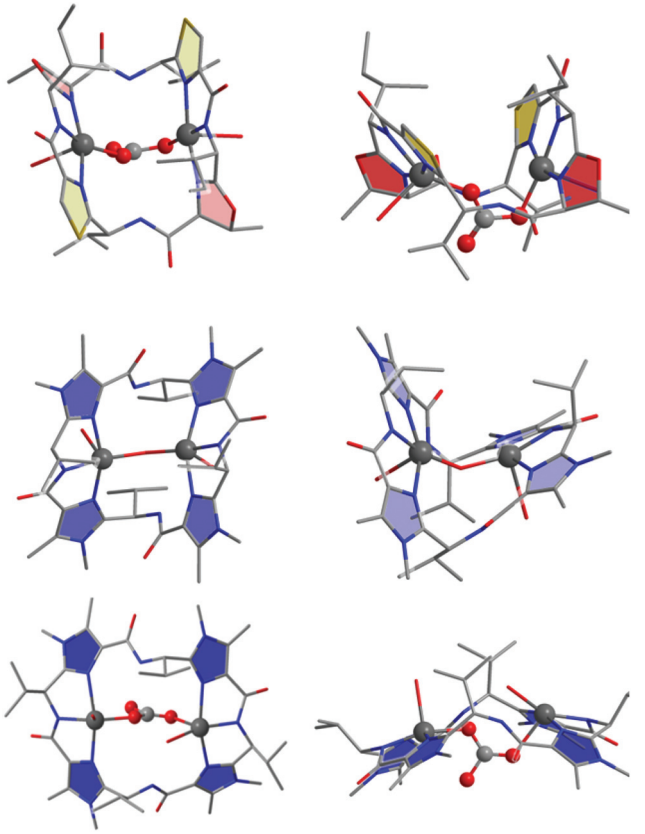

Fig. 12 Structures of the dicopper(II) complexes of H_4asc, H_4pat^1 and H_4pat^2 in top (left) and side views (right); top: $[Cu_2^{II}(H_2asc)(\mu\text{-}CO_3)]$,[34] middle: $[Cu_2^{II}(H_2pat^1)(\mu\text{-}OH)]^+$,[58] bottom: $[Cu_2^{II}(H_2pat^2)(\mu\text{-}CO_3)]$;[56,57] the top two structures are X-ray and the bottom is an MM-DFT-EPR structure. Reproduced by permission of Wiley-VCH from ref. 57.

3.6 Å). Formation of carbonato-bridged complexes with H_4pat^1 could not be observed experimentally so far.[56,57] The substitution of the oxazoline and thiazole heterocycles of patellamides by dimethyl-imidazoles leads to more rigid macrocycles that retain most characteristics of the natural systems (see also section on the structures of the metal-free ligands). In the solid state and in solution the macrocycle H_4pat^1 adopts a conformation very close to that of symmetrical patellamides such as H_4asc. Analysis of the X-ray structures in combination with DFT calculations and spectroscopic investigations showed that the lower flexibility does not strongly influence the preorganization of the macrocycle for the formation of dinuclear Cu^{II} complexes, and this also emerges from the corresponding stability constants (see Table 1).

3.2.3. Reactivities. The formation of carbonato-bridged dicopper(II) complexes indicated that CO_2 hydration might be a function of the *Lissoclinum patella* pseudo-octapeptides. With H_4pat^2 a corresponding complex could be trapped, and its structure was unambiguously determined by EPR spectroscopy together with UV-vis-NIR, CD and MS experiments and combined with DFT-based structure optimization.[59] Interestingly, the structure was determined to be strikingly different to that of $[Cu_2(H_2asc)(1,2\text{-}\mu\text{-}CO_3)(H_2O)_2]$ (see above and Fig. 12; note that the carbonate bridge in the H_4asc system is in the equatorial position for both Cu^{II} centers with a Cu···Cu distance of 3.6 Å, in the H_4pat^2 system the carbonate is bound equatorially to one and axially to the other Cu^{II} center with a Cu···Cu distance of 5.1 Å). It was suggested that a change between various conformations is important to prevent product inhibition in a putative catalytic cycle, and that this depends on the configuration of the macrocycle side-chains and the flexibility of the heterocycles (oxazoline *vs.* imidazole); this was confirmed by preliminary molecular dynamics and Monte-Carlo simulations.[57] Based on ^{13}C and ^{18}O labeling in combination with ESI-MS and NMR experiments, a plausible catalytic cycle was proposed (see Scheme 5), however, catalytic turnover was not shown unambiguously at that stage.[57] The proposed catalytic hydration pathway involves the interaction of CO_2 with one of the Cu^{II} centers and attack of the OH^- nucleophile at the carbon atom of CO_2, leading to a bridging carbonate at the dinuclear active site. ^{13}C and ^{18}O labeling experiments support this mechanistic scenario.[57]

Carbonic anhydrase kinetics are complicated by the fact that a gas is transformed to an ionisable compound, that the solubilities of the species involved in various equilibria strongly depend on solvent, temperature, pressure and pH value, and that all relevant species are colorless (see Scheme 6). Generally, carbonic anhydrase kinetics are measured by stopped-flow techniques, where the time

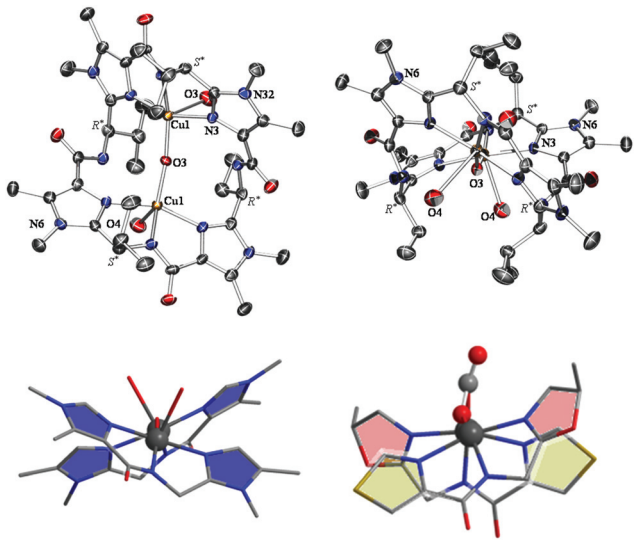

Fig. 13 Top: ORTEP plot of the *S** enantiomer of the crystal structure of the hydroxo-bridged cation $[Cu_2^{II}(H_2pat^1)(\mu\text{-}OH)(H_2O)_2]^+$, top (left) and side view (right). Ellipsoids are drawn at 50% probability, hydrogen atoms and solvent molecules are omitted for clarity; C = grey, N = blue, O = red, Cu = yellow. Bottom: schematic representation of the twist of the binding sites in the hydroxo bridged complex of H_4pat^1 (left) and the carbonato bridged complex of H_4asc (right; dimethylimidazole ring: blue; oxazoline ring: red; thiazole ring: ochre). Reprinted with permission from Inorganic Chemistry from ref. 56. Copyright 2011 by American Chemical Society.

dependence of the color change of a pH indicator is followed, using matched pairs of bases (to capture the protons released from H_2CO_3, see Scheme 6) and indicators.[90,134] It emerges that the pH is not constant during the reaction – for the studies involving the patellamide-type pseudo-octapeptides, there was a change of approx. two pH units under the conditions of the experiments, and this needs to be considered in the analysis of the data. The results, based on the six synthetic pseudo-octapeptides of Scheme 2 and four base/indicator pairs (pK_a values of approx. 6.2, 7.1, 8.1, 8.2) are presented in Table 2.[23,34,43,56,57,90,93,94] It follows that all six patellamide-based dicopper(II) complexes are very efficient carbonic anhydrase catalysts with maximum efficiency using Tris [(tris-hydroxymethyl)-aminomethane, pK_a = 8.07] as base, with a turnover number (TON) of at least 1700 (limited only by the amount of base used) and a catalytic rate between 1.7×10^3 and 7.3×10^3 s^{-1}. The rate of the uncatalyzed hydration of CO_2 at 25° is 3.7×10^{-2} s^{-1},[134,135] *i.e.* there is an approx. 10^5-fold acceleration by the dicopper(II)–patellamide catalysts, and this is only approx. 2 orders of magnitude slower than the enzymes (2×10^5–1.4×10^6 s^{-1});[134,136] rates of other model systems generally are smaller (1×10^2–5×10^3 s^{-1}, typically in the pH range of 7–9),[137] and the systems discussed here are the most efficient CO_2 hydration catalysts known so far. Very interestingly, the synthetic analogue H_4pat^1, where we have not been able to trap a carbonato-bridged complex, is the most efficient catalyst studied, more efficient than H_4L^{ascA}, the structurally most similar model of H_4asc.[23,34,43,56,57,90,93,94] This is in agreement with the mechanistic scenario shown in Scheme 6 and rate-determining nucleophilic attack at the CO_2 carbon atom coordinated to one of the Cu^{II} centers by the hydroxo group coordinated to the other Cu^{II} center. It also indicates that partial inhibition by product (carbonate or bicarbonate) coordination can decrease the catalytic efficiency, and this seems to be linked to the configuration of the peptide side-chains, where the natural (mixed) configuration in H_4L^{ascA} and H_4pat^1 lead, as expected,[58] to little inhibition (this is supported by the fact that so far no carbonato-bridged species was observed with H_4pat^1, see above).

The efficient dicopper(II)-cyclic pseudo-octapeptide catalyzed "hydrolysis" of CO_2 indicated that other similar reactions might be possible, and that of phosphoesters, *i.e.* phosphatase-type activity, seemed to be a reasonable option to test.[88] The dicopper(II) complex of H_4pat^1 was tested with the usual substrates [bis(2,4-dinitrophenyl)phosphate, BDNPP, as a phosphodiester, and 2,4-dinitrophenylphosphate, DNPP, as a phosphomonoester in H_2O : MeCN : MeOH = 50 : 45 : 5 (solubility); other conditions are given in the caption to Fig. 14].[58] Indeed, the patellamide–dicopper(II) complexes are very efficient phosphatase mimics for phosphodiesters, and the bell-shaped dependence of the rate from pH indicates that a mechanism similar to that proposed for purple acid phosphatases (PAP) applies, *i.e.* the phosphoester coordinates to the copper site with a coordinated H_2O and is attacked by the hydroxide nucleophile coordinated to the other copper center – this is also consistent with the expected pK_a values of H_2O coordinated to the two copper(II) centers and the corresponding observations with the CO_2 hydration reactivity, see above (Scheme 7, Fig. 14).[88] An interesting observation is that $[Cu_2^{II}(H_2pat^1)(OH)(H_2O)]^+$ also efficiently catalyzes the hydrolysis of the monoester DNPP. Although this is the biological role of purple acid phosphatases,[58] it was only recently that low molecular weight mimics were first shown to be able to fulfil this requirement.[138,139] In these diiron PAP model systems, the monoesterase activity was achieved by carefully designed secondary interactions (H-bonding networks) which prevented bridging geometries of the monoester and phosphate substrates and products. It appears that the conformational flexibility of the patellamide–dicopper systems fulfils a similar role (see carbonic anhydrase activity discussed above) but at this moment this is only a speculation which needs to be substantiated with further studies.

3.3. Possible biological functions

The metabolic role of the cyclic pseudo-peptides is unknown, even metal ion coordination, specifically that of Cu^{II}, which has been studied *in vitro* in much detail in recent years, has not been supported by biochemical studies. Nevertheless, a number of observations indicate that Cu^{II} coordination might be of importance and Cu^{II} storage and transport, CO_2 fixation, Cu_2^{II} transport and phosphatase activity as well as oxygen activation – specifically if the cyclic peptides should be prosthetic groups in peptides – have been discussed as possible biological functions (note that possible natural roles have primarily

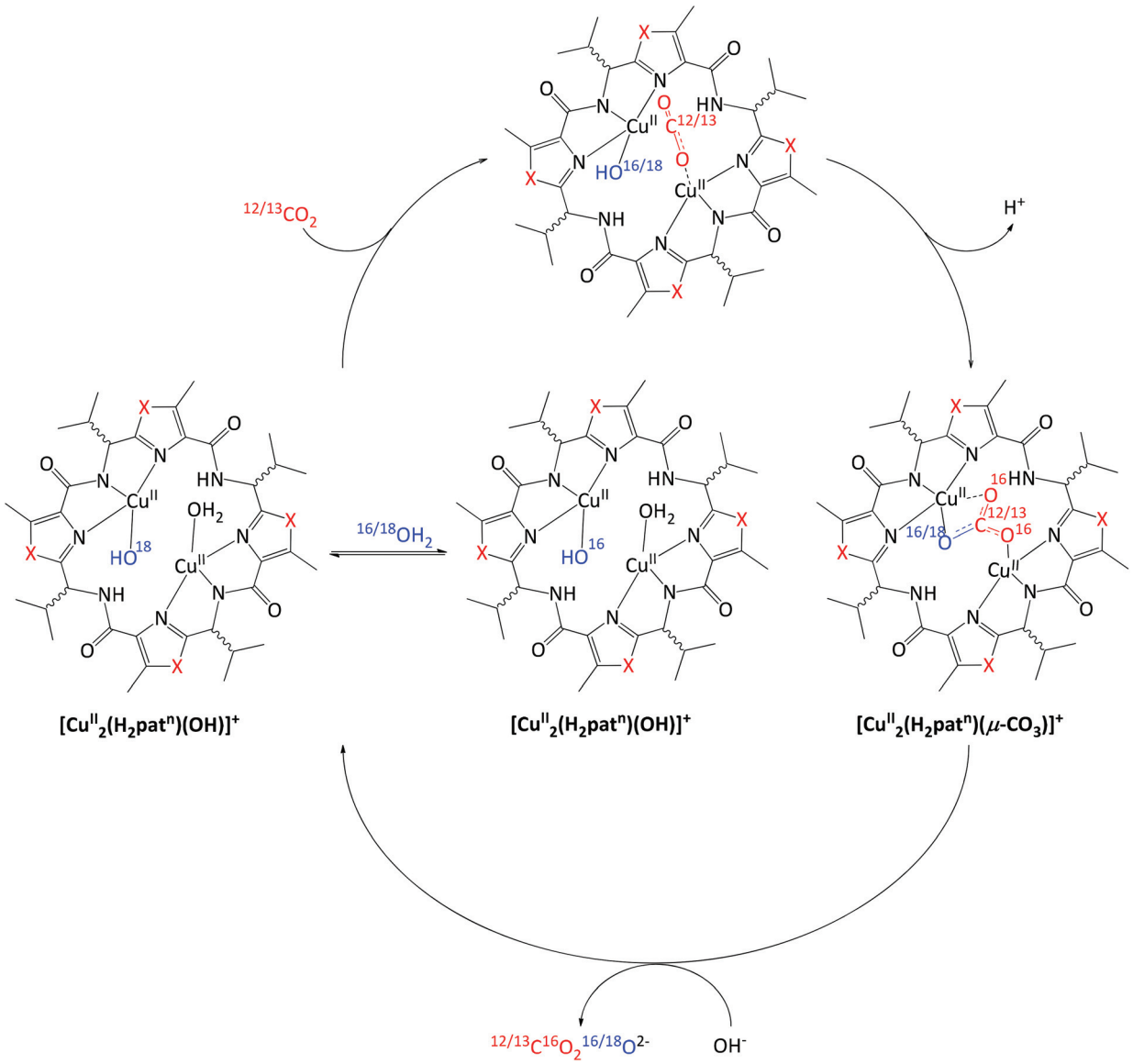

Scheme 5 $[Cu^{II}(H_2pat^n)(OH)]^+$ catalyzed hydration of CO_2: carbonic anhydrase activity. Reproduced from ref. 90.

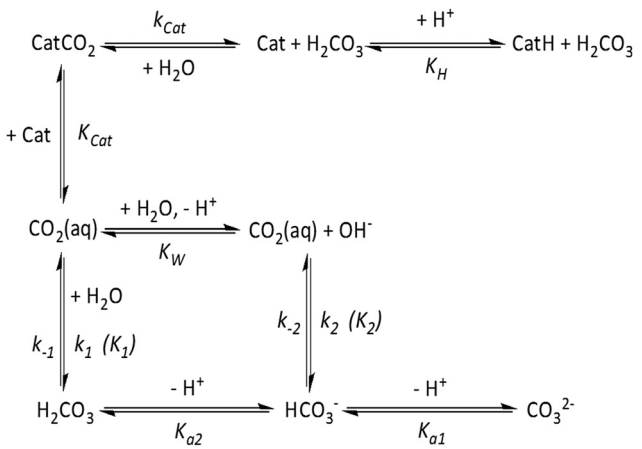

Scheme 6 Equilibria involved in the hydration of CO_2. The catalyst (Cat) corresponds to the dinuclear $[Cu^{II}(H_2pat^n)(OH)]^+$ complex. Reproduced from ref. 90.

been discussed for the patellamide/ascidiacyclamide-type pseudo-octapeptides, the corresponding westiellamide-type pseudo-hexapeptides and the other macrocycles shown in Scheme 1 have not been considered in detail so far).[34,56–58,88,91,138] It is of interest that recent preliminary experiments of the corresponding Zn^{II} complexes[122] indicate not unexpectedly that these also are efficient catalyst for phosphoester hydrolysis,[140] and we anticipate that they will also show carbonic anhydrase activity. Another set of preliminary experiments indicates that interesting vanadium chemistry is to be expected – and this is relevant due to the known affinity of the ascidians for V^{III}. It also appears that, apart from CO_2 hydration (and its reverse of course) and phosphatase activity, other biologically relevant hydrolysis reactions might be catalyzed by metal complexes of the cyclic peptides. It is quite evident that interesting experimental data combined with theory-based studies will help to complete the current picture

Table 2 Hydration rates of CO_2, catalyzed by the dicopper(II) complexes of the six analogues of the patellamides given in Scheme 2,[90] (k_{cat}; reactions with 8.5 mmol base, 17 mmol CO_2, 5 μmol catalyst, 12.5 μmol indicator, in a water–methanol 9 : 1 at 25 °C; analysis based on parameters from the literatur, see ref 90 for details; average and standard deviation of 5 independent measurements)

	k_{cat} [s^{-1}]			
Ligand	pK_a 6.21	pK_a 7.14	pK_a 8.07	pK_a 8.22
H_4pat^1	$1.71 \times 10^{-3} \pm 9.09 \times 10^{-4}$	$7.08 \times 10^{1} \pm 2.32 \times 10^{0}$	$7.32 \times 10^{3} \pm 3.65 \times 10^{2}$	$6.00 \times 10^{2} \pm 1.75 \times 10^{2}$
H_4pat^2	$1.54 \times 10^{-3} \pm 1.26 \times 10^{-3}$	$6.96 \times 10^{1} \pm 1.41 \times 10^{0}$	$1.72 \times 10^{3} \pm 1.05 \times 10^{2}$	$1.15 \times 10^{2} \pm 1.28 \times 10^{1}$
H_4pat^3	$1.10 \times 10^{-3} \pm 9.35 \times 10^{-4}$	$7.32 \times 10^{1} \pm 6.04 \times 10^{0}$	$1.86 \times 10^{3} \pm 8.00 \times 10^{1}$	$1.18 \times 10^{2} \pm 3.80 \times 10^{1}$
H_4pat^4	$2.27 \times 10^{-3} \pm 1.25 \times 10^{-3}$	$7.74 \times 10^{1} \pm 1.62 \times 10^{1}$	$1.92 \times 10^{3} \pm 1.10 \times 10^{2}$	$1.12 \times 10^{2} \pm 2.20 \times 10^{1}$
H_4pat^5	$1.94 \times 10^{-3} \pm 1.32 \times 10^{-3}$	$7.25 \times 10^{1} \pm 2.63 \times 10^{0}$	$2.05 \times 10^{3} \pm 2.91 \times 10^{1}$	$1.11 \times 10^{2} \pm 1.63 \times 10^{1}$
H_4L^{ascA}	$1.41 \times 10^{-3} \pm 1.14 \times 10^{-3}$	$7.49 \times 10^{1} \pm 4.55 \times 10^{0}$	$4.68 \times 10^{3} \pm 2.04 \times 10^{2}$	$2.59 \times 10^{2} \pm 2.30 \times 10^{1}$

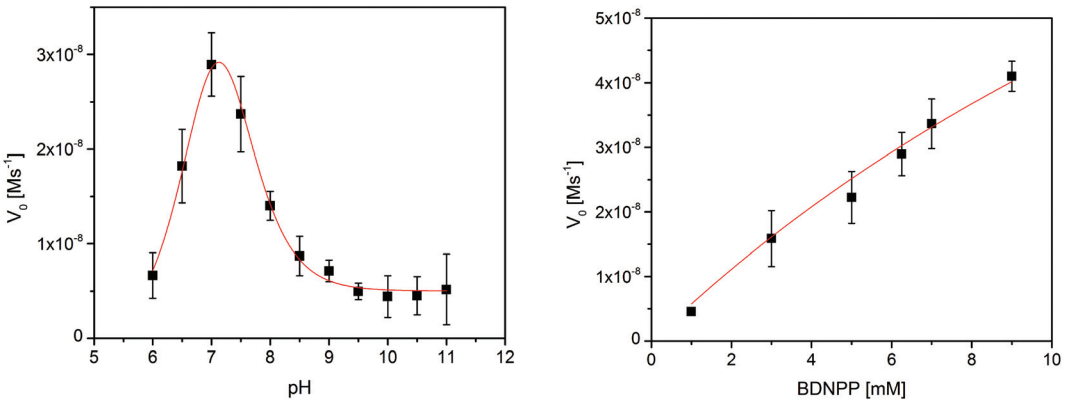

Fig. 14 pH- and BDNPP concentration dependence of the $[Cu^{II}_2(H_2pat^1)(\mu\text{-}OH)(H_2O)_2]^+$-catalyzed BDNPP hydrolysis (error bars are standard deviations obtained from fits of the relevant Michaelis–Menton equations);[88] catalyst concentration: 40 μM, BDNPP for the pH dependence: 6.25 mM, pH for the substrate dependence: 7.06, μ = 0.45; pH_{max} = 7.21; pK_a^{I} = 6.91 ± 0.21, pK_a^{II} = 7.31 ± 0.20 (in our mechanistic model, these correspond to the pK_a values of the two coordinated OH_2 molecules); K_M = (26.4 ± 2.20) mM; k_{cat} = (3.95 ± 0.07) × 10^{-3} s^{-1}; k_{cat}/K_M = 0.15 ± 0.03). Reproduced from ref. 88.

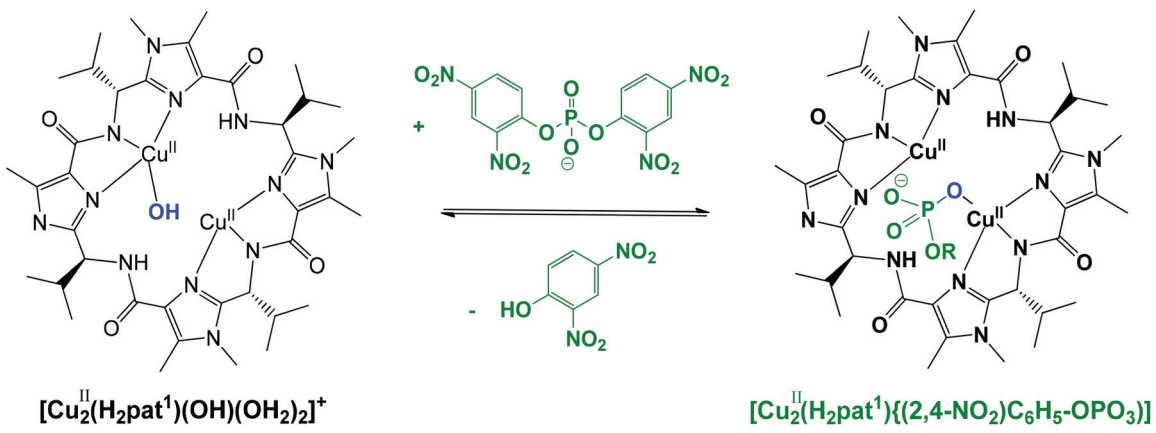

Scheme 7 $[Cu^{II}(H_2pat^1)(OH)]^+$ catalyzed phosphoester hydrolysis: phosphatase reactivity.[88]

of the reactivities of natural and synthetic cyclic pseudo-peptide ligands coordinated to metal ions. However, for an unambiguous answer to the question, what the biological role of these interesting natural products is, their biochemistry needs to be studied.

4. Conclusions

The issues raised in a 1993 review of marine metabolites and metal ion chelation, *i.e.* the availability of the cyclic pseudo-peptides and their metal complexes, an unambiguous

characterization of the relevant structures and the analysis of possible reactivities of the metal complexes in relation to their putative biological activities,[112] have been addressed with some success in the last two decades. The syntheses of cyclic pseudo-peptides, although still time consuming, have been developed to an extent, where, particularly for the peptides based on the *L. patella* families, there now are methods which allow a relatively large variety of these macrocyclic ligands to be obtained in respectable yields utilising tedious but efficient procedures. Their stereochemical and solution structural assignments have now become routine. The suggestion that molecular mechanics studies should assume greater importance has proved to be valuable;[112] of particular importance, specifically for the Cu^{II} complexes and the relatively complex solution equilibria in which they are involved, was the combination of various experimental and theory-based structural and spectroscopic approaches – a methodology that has been shown to be of importance in transition metal coordination chemistry in general.[141] The issue of the relevance of the metal complexes for the biological activity of the peptides remains largely unresolved although recent developments in terms of the carbonic anhydrase and phosphatase chemistry of the Cu^{II} complexes are providing an interesting and potentially significant advance.

The break-through in our own studies was the accessibility of a variety of ligands based on a modular synthesis which allowed the preparation of appreciable quantities of ligands in relatively short time, and with the possibility to tune their structures and flexibilities as well as the electronics of the donor groups *via* the type of heterocycle and the configuration of the macrocycle side-chain.[54,56,57,65,66,68] The other important factor, leading to a comprehensive account with respect to the coordination chemistry involved, is based on the combination of various spectroscopies (UV-vis-NIR, CD, MCD, ESI-MS, NMR, EPR, HYSCORE and ENDOR) with computational modeling (structure optimization and electronic structure calculation); thorough kinetic studies and thermodynamic analyses have started to appear and begin also to be combined with modeling approaches – in this area there still is important work ahead. Obvious next steps are similar sets of experiments with other metal ions and other (hydrolysis) reactions. Preliminary experiments indicate that the corresponding Zn^{II} complexes are also efficient phosphatase models and that stable vanadium complexes are available.[140] Extension of these experiments might lead to interesting and possibly important new avenues. However, *the* important and demanding question remains: are the observed reactivities (carbonic anhydrase, phosphatase and others) related to the biological function of these fascinating natural products?

Acknowledgements

We are grateful for generous financial support by the German Science Foundation (DFG) the German Academic Exchange Servic (DAAD), the University of Heidelberg and the University of Queensland.

References

1 R. F. Nigrelli, S. Jakowska and I. Calventi, *Zoologica*, 1959, **44**, 173–174.
2 S. Jakowska and R. F. Nigrelli, *Ann. N. Y. Acad. Sci.*, 1960, **90**, 913–916.
3 M. R. Schmeer and C. V. Huala, *Ann. N. Y. Acad. Sci.*, 1960, **90**, 893.
4 P. R. Burkholder and L. M. Burkholder, *Science*, 1960, **127**, 1174.
5 C. P. Li, B. Prescott and W. B. Jahnes, *Proc. Natl. Acad. Sci. U. S. A.*, 1962, **109**, 534.
6 R. F. Nigrelli, M. F. Stempien, G. D. Ruggieri, V. R. Ligouri and J. T. Cecil, *Fed. Proc.*, 1967, **26**, 1197.
7 C. M. Ireland, B. R. Copp, M. P. Foster, L. A. McDonald, D. C. Radisky and J. C. Swersey, *Marine Biotechnology, Volume 1: Pharmaceutical and Bioactive Natural Products*, Plenum Press, New York, 1992.
8 B. S. Davidson, *Chem. Rev.*, 1993, **93**, 1771–1791.
9 D. J. Faulkner, *Nat. Prod. Rep.*, 1988, **5**, 613–663.
10 J. R. Lewis, *Nat. Prod. Rep.*, 1989, **6**, 503–513.
11 N. Fusetani, T. Sugawara, S. Matsunaga and H. Hirota, *J. Am. Chem. Soc.*, 1991, **113**, 7811–7812.
12 G. Abbenante, D. R. March, D. A. Bergman, P. A. Hunt, B. Garnham, R. J. Dancer, J. L. Martin and D. P. Fairlie, *J. Am. Chem. Soc.*, 1995, **117**, 10220–10226.
13 H. C. Krebs, in *Progress in the Chemistry of Organic Natural Products*, Springer, Wien, 1986, pp. 151–363.
14 M. K. Rosen and S. L. Schreiber, *Angew. Chem., Int. Ed.*, 1992, **31**, 384–400.
15 N. Fuesetani, in *Drugs from the Sea*, ed. M. Fuesetani, Karger, Basel, 2000, ch. 1, pp. 1–5.
16 S. Chakraborty and U. Ghosh, *J. Pharm. Res.*, 2010, **3**, 1293–1296.
17 B. M. Degnan, C. J. Hawkins, M. F. Lavin, E. J. McCaffrey, D. L. Parry and D. J. Watters, *J. Med. Chem.*, 1989, **32**, 1354–1359.
18 B. F. Milne, P. F. Long, A. Starcevic, D. Hranueli and M. Jaspars, *Org. Biomol. Chem.*, 2006, **4**, 631–638.
19 G. Abbenante, D. P. Fairlie, L. R. Gahan, G. R. Hanson, G. K. Pierens and A. L. van den Brenk, *J. Am. Chem. Soc.*, 1996, **118**, 10384–10388.
20 P. F. Long, W. C. Dunlap, C. N. Battershill and M. Jaspars, *ChemBioChem*, 2005, **6**, 1760–1765.
21 E. W. Schmidt, J. T. Nelson, D. A. Rasko, S. Sudek, J. A. Eisen, M. G. Haygood and J. Ravel, *Proc. Natl. Acad. Sci. U. S. A.*, 2005, **102**, 7315–7320.
22 N. Withers, W. Vidaver and R. A. Lewin, *Phycologia*, 1978, **17**, 167–171.
23 M. Kühl and A. W. D. Larkum, in *Cellular Origin and Life in Extreme Habitats*, ed. J. Seckbach, Kluwer Acad. Publ., Dordrecht, 2002, vol. 3, Symbiosis, Mechanisms and Model Systems, pp. 273–290.
24 A. Shimada, N. Yano, S. Kanai, R. A. Lewin and T. Maruyama, *Phycologia*, 2003, **42**, 193–197.

25 J. M. Wasylyk, J. E. Biskupiak, C. E. Costello and C. M. Ireland, *J. Org. Chem.*, 1983, **48**, 4445–4449.
26 B. M. Degnan, C. J. Hawkins, M. F. Lavin, E. J. McCaffrey, D. L. Parry, A. L. van den Brenk and D. J. Watters, *J. Med. Chem.*, 1989, **32**, 1349–1354.
27 F. J. Schmitz, M. B. Ksebati, J. S. Chang, J. L. Wang, M. B. Hossain, D. Van der Helm, M. H. Engel, A. Serban and J. A. Silfer, *J. Org. Chem.*, 1989, **54**, 3463–3472.
28 C. J. Hawkins, M. F. Lavin, K. A. Marshall, A. L. van den Brenk and D. J. Watters, *J. Med. Chem.*, 1990, **33**, 1634–1638.
29 L. A. Morris, J. J. K. van den Bosch, K. Versluis, G. S. Thompson and M. Jaspars, *Tetrahedron*, 2000, **56**, 8345–8353.
30 C. M. Ireland, A. R. Durso Jr., R. A. Newman and M. P. Hacker, *J. Org. Chem.*, 1982, **47**, 1807–1811.
31 M. A. Rashid, K. R. Gustafson, J. H. Cardellina and M. R. Boyd, *J. Nat. Prod.*, 1995, **58**, 594–597.
32 L. A. Mcdonald and C. M. Ireland, *J. Nat. Prod.*, 1992, **55**, 376–379.
33 Y. Hamamoto, M. Endo, M. Nakagawa, T. Nakanishi and K. Mizukawa, *J. Chem. Soc., Chem. Commun.*, 1983, 323–324.
34 A. L. van den Brenk, K. A. Byriel, D. P. Fairlie, L. R. Gahan, G. R. Hanson, C. J. Hawkins, A. Jones, C. H. L. Kennard, B. Moubaraki and K. S. Murray, *Inorg. Chem.*, 1994, **33**, 3549–3557.
35 M. R. Prinsep, R. E. Moore, I. A. Levine and G. M. L. Patterson, *J. Nat. Prod.*, 1992, **55**, 140–142.
36 T. W. Hambley, C. J. Hawkins, M. F. Lavin, A. van den Brenk and D. J. Watters, *Tetrahedron*, 1992, **48**, 341–348.
37 L. J. Perez and D. J. Faulkner, *J. Nat. Prod.*, 2003, **66**, 247–250.
38 C. G. Shin, C. Abe and Y. Yonezawa, *Chem. Lett.*, 2004, 664–665.
39 Y. Nakamura and S. Takeuchi, *QSAR Comb. Sci.*, 2006, **25**, 703–708.
40 M. P. Foster, G. P. Concepcion, G. B. Caraan and C. M. Ireland, *J. Org. Chem.*, 1992, **57**, 6671–6675.
41 F. Ikegami and I. Murakoshi, *Phytochemistry*, 1994, **35**, 1089–1104.
42 M. Wang and S. J. Gould, *J. Org. Chem.*, 1993, **58**, 5176–5180.
43 L. A. Morris and M. Jaspers, in *A Cu^{2+} selective marine metabolite*, RSC Special Publications, 2000, vol. 257, pp. 140–166.
44 L. A. Morris, M. Jaspars, J. J. Kettenes-van den Bosch, K. Versluis, A. J. R. Heck, S. M. Kelly and N. C. Price, *Tetrahedron*, 2001, **57**, 3185–3197.
45 L. A. Morris, B. F. Milne, M. Jaspars, J. J. Kettenes-van den Bosch, K. Versluis, A. J. R. Heck, S. M. Kelly and N. C. Price, *Tetrahedron*, 2001, **57**, 3199–3207.
46 A. L. van den Brenk, G. R. Hanson and C. J. Hawkins, *J. Inorg. Biochem.*, 1989, **98**, 165.
47 P. Wipf, S. Venkatraman, C. P. Miller and S. J. Geib, *Angew. Chem., Int. Ed.*, 1994, **33**, 1516–1518.
48 P. Comba, R. Cusack, D. P. Fairlie, L. R. Gahan, G. R. Hanson, U. Kazmaier and A. Ramlow, *Inorg. Chem.*, 1998, **37**, 6721–6727.
49 L. A. Morris, B. F. Milne, G. S. Thompson and M. Jaspars, *J. Chem. Soc., Perkin Trans. 2*, 2002, 1072–1075.
50 A. L. van den Brenk, J. D. A. Tyndall, R. M. Cusack, A. Jones, D. P. Fairlie, L. R. Gahan and G. R. Hanson, *J. Inorg. Biochem.*, 2004, **98**, 1857–1866.
51 P. Wipf and C. B. Wang, *Org. Lett.*, 2006, **8**, 2381–2384.
52 F. Boitel and J. P. Truchot, *Mar. Biol.*, 1989, **103**, 495–501.
53 P. V. Bernhardt, P. Comba, D. P. Fairlie, L. A. Gahan, G. R. Hanson and L. Lötzbeyer, *Chem.–Eur. J.*, 2002, **8**, 1527–1536.
54 P. Comba, L. R. Gahan, G. Haberhauer, G. R. Hanson, C. J. Noble, B. Seibold and A. L. van den Brenk, *Chem.–Eur. J.*, 2008, **14**, 4393–4403.
55 P. Comba, N. Dovalil, G. Haberhauer, G. R. Hanson, Y. Karod and T. Taura, *J. Biol. Inorg. Chem.*, 2010, **15**, 1129–1135.
56 P. Comba, N. Dovalil, G. R. Hanson and G. Linti, *Inorg. Chem.*, 2011, **50**, 5165–5174.
57 P. Comba, N. Dovalil, L. R. Gahan, G. Haberhauer, G. R. Hanson, C. J. Noble, B. Seibold and P. Vadivelu, *Chem.–Eur. J.*, 2012, **18**, 2578–2590.
58 G. Schenk, N. Mitic, G. Hanson and P. Comba, *Coord. Chem. Rev.*, 2012, 473–482.
59 P. Comba, N. Dovalil, G. Haberhauer, G. R. Hanson, J. Harmer, C. J. Noble, M. J. Riley and B. Seibold, publication in preparation.
60 W. E. Houssen and M. Jaspars, *ChemBioChem*, 2010, **11**, 1803–1815.
61 A. Bertram and G. Pattenden, *Nat. Prod. Rep.*, 2007, **24**, 18–30.
62 W. E. Houssen, J. Koehnke, D. Zollman, J. Vendome, A. Raab, M. C. M. Smith, J. H. Naismith and M. Jaspars, *ChemBioChem*, 2012, **13**, 2683–2689.
63 J. Koehnke, A. Bent, W. E. Houssen, D. Zollman, F. Morawitz, S. Shirran, J. Vendome, A. F. Nneoyiegbe, L. Trembleau, C. H. Botting, M. C. M. Smith, M. Jaspars and J. H. Naismith, *Nat. Struct. Mol. Biol.*, 2012, **19**, 767–773.
64 P. Wipf, C. P. Miller and C. M. Grant, *Tetrahedron*, 2000, **56**, 9143–9150.
65 G. Haberhauer and F. Rominger, *Eur. J. Org. Chem.*, 2003, 3209–3218.
66 G. Haberhauer, A. Pinter, T. Oeser and F. Rominger, *Eur. J. Org. Chem.*, 2007, 1779–1792.
67 P. Wipf and C. Wang, *Org. Lett.*, 2006, **8**, 2381–2384.
68 G. Haberhauer, *Tetrahedron Lett.*, 2008, **49**, 2421.
69 Azole: class of five-membered nitrogen heterocyclic ring compounds containing at least one other non-carbon atom of either nitrogen, sulfur, or oxygen.
70 Y. Hamada, M. Shibata and T. Shioiri, *Tetrahedron Lett.*, 1985, **26**, 5159–5162.
71 Y. Hamada, M. Shibata and T. Shioiri, *Tetrahedron Lett.*, 1985, **26**, 5155–5158.

72 T. Ishida, Y. In, F. Shinozaki, M. Doi, D. Yamamoto, Y. Hamada, T. Shioiri, M. Kamigauchi and M. Sugiura, *J. Org. Chem.*, 1995, **60**, 3944–3952.
73 T. Ishida, Y. In, M. Doi, M. Inoue, Y. Hamada and T. Shioiri, *Biopolymers*, 1992, **32**, 131–143.
74 Y. In, M. Doi, M. Inoue, T. Ishida, Y. Hamada and T. Shioiri, *Chem. Pharm. Bull.*, 1993, **41**, 1686–1690.
75 Y. In, M. Doi, M. Inoue and T. Ishida, *Acta Crystallogr., Sect. C: Cryst. Struct. Commun.*, 1994, **50**, 2015–2017.
76 R. M. Cusack, L. Grondahl, G. Abbenante, D. P. Fairlie, L. R. Gahan, G. R. Hanson and T. W. Hambley, *J. Chem. Soc., Perkin Trans. 2*, 2000, 323–331.
77 B. F. Milne, L. A. Morris, M. Jaspars and G. S. Thompson, *J. Chem. Soc., Perkin Trans. 2*, 2002, 1076–1080.
78 G. Haberhauer and F. Rominger, *Tetrahedron Lett.*, 2002, **43**, 6335–6338.
79 G. Haberhauer, T. Oeser and F. Rominger, *Chem. Commun.*, 2005, 2799–2801.
80 G. Haberhauer, A. Pinter, T. Oeser and F. Rominger, *Eur. J. Org. Chem.*, 2007, 1779–1792.
81 G. Haberhauer, E. Drosdow, T. Oeser and F. Rominger, *Tetrahedron*, 2008, **64**, 1853–1859.
82 A. Pinter and G. Haberhauer, *Tetrahedron*, 2009, **65**, 2217–2225.
83 G. Haberhauer and A. Pinter, in *Modeling of Molecular Properties*, ed. P. Comba, Wiley-VCH, Weinheim, 2011, pp. 365–396.
84 T. Ishida, M. Inoue, Y. Hamada, S. Kato and T. Shioiri, *J. Chem. Soc., Chem. Commun.*, 1987, 370–371.
85 F. Shinozaki, Y. In, M. Doi, D. Yamamoto, M. Kamigauchi, M. Sugiura, T. Ishida, Y. Hamada and T. Shioiri, *Pept. Chem.*, 1996, **34th**, 405–408.
86 P. Wipf and C. P. Miller, *J. Am. Chem. Soc.*, 1992, **114**, 10975–10977.
87 P. Wipf, *Alkaloids: Chemical and Biological Perspectives*, Pergamon, New York, 1998.
88 P. Comba, L. R. Gahan, G. R. Hanson and M. Westphal, *Chem. Commun.*, 2012, 9364–9366.
89 P. Comba, N. Dovalil, G. Haberhauer, K. Kowski, N. Mehrkens and M. Westphal, *Z. Allg. Anorg. Chem.*, 2013, **639**, 1395–1400 (*Special Issue Bioinorganic Chemistry*).
90 P. Comba, L. R. Gahan, G. R. Hanson, M. Maeder and M. Westphal, *Dalton Trans.*, 2013, submitted.
91 R. Latifi, M. Bagherzadeh, B. F. Milne, M. Jaspars and S. P. De Visser, *J. Inorg. Biochem.*, 2008, **102**, 2171–2178.
92 S. H. Wright, A. Raab, J. Feldmann, E. Krupp and M. Jaspers, in *Handbook of Marine Natural Products*, ed. E. Fattorusso, W. H. Gerwick and O. Taglialatela-Scatati, Springer, Heidelberg, New York, 2012, pp. 861–892.
93 B. P. Kremer, R. Pardy and R. A. Lewin, *Phycologia*, 1982, **21**, 258–263.
94 A. L. van den Brenk, D. P. Fairlie, G. R. Hanson, L. R. Gahan, C. J. Hawkins and A. Jones, *Inorg. Chem.*, 1994, **33**, 2280–2289.
95 Y.-M. Li, J. C. Milne, L. L. Madison, R. Kolter and C. T. Walsh, *Science*, 1996, **274**, 1188–1193.
96 P. Wipf, P. C. Fritch, S. J. Geib and A. M. Sefler, *J. Am. Chem. Soc.*, 1998, **120**, 4105–4112.
97 G. Haberhauer, T. Oeser and F. Rominger, *Chem.–Eur. J.*, 2005, **11**, 6718–6726.
98 M. Schnopp, S. Ernst and G. Haberhauer, *Eur. J. Org. Chem.*, 2009, 213–222.
99 K. A. Jolliffe, *Supramol. Chem.*, 2005, **17**, 81–86.
100 V. J. Dungan, H. T. Ngo, P. G. Young and K. A. Jolliffe, *Chem. Commun.*, 2013, **49**, 264–266.
101 M. Schnopp and G. Haberhauer, *Eur. J. Org. Chem.*, 2009, 4458–4467.
102 Y. Singh, N. Sokolenko, M. J. Kelso, L. R. Gahan, G. Abbenante and D. P. Fairlie, *J. Am. Chem. Soc.*, 2001, **123**, 333–334.
103 D. Mink, S. Mecozzi and J. Rebek, *Tetrahedron Lett.*, 1998, **39**, 5709–5712.
104 A. Pinter and G. Haberhauer, *Synlett*, 2009, 3082–3098.
105 C. Tepper and G. Haberhauer, *Beilstein J. Org. Chem.*, 2012, **8**, 977–985.
106 C. Tepper and G. Haberhauer, *Chem.–Eur. J.*, 2011, **29**, 8060–8065.
107 G. Haberhauer, *Angew. Chem., Int. Ed.*, 2011, **50**, 6415–6418.
108 G. Haberhauer, *Angew. Chem., Int. Ed.*, 2010, **49**, 9286–9289.
109 T. Ishida, M. Tanaka, M. Nabae, M. Inoue, S. Kato, Y. Hamada and T. Shioiri, *J. Org. Chem.*, 1988, **53**, 107–112.
110 C. J. Hawkins, *Pure Appl. Chem.*, 1988, **60**, 1267–1270.
111 R. Latifi, M. Bagherzadeh, B. F. Milne, M. Jaspars and S. P. de Visser, *J. Inorg. Biochem.*, 2008, **102**, 2171–2178.
112 J. P. Michael and G. Pattenden, *Angew. Chem., Int. Ed. Engl.*, 1993, **32**, 1–23.
113 D. J. Freeman, G. Pattenden, A. F. Drake and G. Siligardi, *J. Chem. Soc., Perkin Trans. 2*, 1998, 129–135.
114 I. Sovago, C. Kallay and K. Varnagy, *Coord. Chem. Rev.*, 2012, **256**, 2225–2233.
115 I. Sovago and K. Ösz, *Dalton Trans.*, 2006, 3841–3854.
116 I. Sovago, D. Sanna, A. Dessi, K. Varnagy and G. Micera, *J. Inorg. Biochem.*, 1996, **63**, 99–117.
117 M. Atanasov, P. Comba, B. Martin, V. Müller, G. Rajaraman, H. Rohwer and S. Wunderlich, *J. Comput. Chem.*, 2006, **27**, 1263.
118 C. Ireland and P. J. Scheuer, *J. Am. Chem. Soc.*, 1980, **102**, 5688–5691.
119 Y. Hamada, S. Kato and T. Shioiri, *Tetrahedron Lett.*, 1985, **26**, 3223–3226.
120 L. A. Morris, M. Jaspars, J. J. K.-v. d. Bosch, K. Versluis, A. J. R. Heck, S. M. Kelly and N. C. Price, *Tetrahedron*, 2001, **57**, 3185–3197.
121 A. Bertram and G. Pattenden, *Nat. Prod. Rep.*, 2007, **24**, 18.
122 L. Grondahl, N. Sokolenko, G. Abberate, D. P. Fairlie, G. R. Hanson and L. R. Gahan, *J. Chem. Soc., Dalton Trans.*, 1999, 1227–1234.

123 R. M. Cusack, L. Grondahl, D. P. Fairlie, L. R. Gahan, G. R. Hanson and G. R. Hanson, *J. Chem. Soc., Perkin Trans. 2*, 2002, 556–563.
124 A. L. van den Brenk, D. P. Fairlie, L. R. Gahan, G. R. Hanson and T. W. Hambley, *Inorg. Chem.*, 1996, **35**, 1095–1100.
125 Note that, due to problems with the solubility of the ligands and/or complexes in water, most of our and other groups' experiments are done in pure MeOH or MeOH–water mixtures. Note also that quite generally (and if not mentioned otherwise), our experiments were done under exclusion of air.
126 T. D. Smith and J. R. Pilbrow, *Coord. Chem. Rev.*, 1974, **13**, 173–278.
127 G. R. Hanson, C. J. Noble and S. Benson, *Biol. Magn. Reson.*, 2009, **28**, 105–173.
128 P. V. Bernhardt, P. Comba, T. W. Hambley, S. S. Massoud and S. Stebler, *Inorg. Chem.*, 1992, **31**, 2644–2651.
129 P. Comba, Y. D. Lampeka, A. Prikhod'ko and G. Rajaraman, *Inorg. Chem.*, 2006, **45**, 3632–3638.
130 M. Atanasov, P. Comba and C. A. Daul, *Inorg. Chem.*, 2008, **47**, 2449.
131 P. Comba, S. Hausberg and B. Martin, *J. Phys. Chem. A*, 2009, **113**, 6751.
132 M. Atanasov, P. Comba, G. R. Hanson, S. Hausberg, S. Helmle and H. Wadepohl, *Inorg. Chem.*, 2011, **50**, 6890–6901.
133 A. Bentz, P. Comba, R. J. Deeth, M. Kerscher, H. Pritzkow, B. Seibold and H. Wadepohl, *Inorg. Chem.*, 2008, **47**, 9518.
134 R. G. Kalifah, *J. Biol. Chem.*, 1971, **246**, 2561–2573.
135 X. Wang, W. Conway, R. Burns, N. McCann and M. Maeder, *J. Phys. Chem. A*, 2010, **114**, 1734–1740.
136 J. C. Kernohan, *Biochim. Biophys. Acta*, 1965, **96**, 304.
137 D. A. Palmer and R. van Eldik, *Chem. Rev.*, 1983, **83**, 651–731.
138 P. Comba, L. R. Gahan, G. R. Hanson, V. Mereacre, C. J. Noble, A. K. Powell, I. Prisecaru, G. Schenk and M. Zajaczkowski-Fischer, *Chem.–Eur. J.*, 2012, **18**, 1700–1710.
139 P. Comba, L. R. Gahan, V. Mereacre, G. R. Hanson, A. K. Powell, G. Schenk and M. Zajaczkowski-Fischer, *Inorg. Chem.*, 2012, **51**, 12195–12209.
140 P. Comba, N. Mehrkens and M. Westphal, Work in progress.
141 P. Comba and M. Kerscher, *Coord. Chem. Rev.*, 2009, **253**, 564–574.

